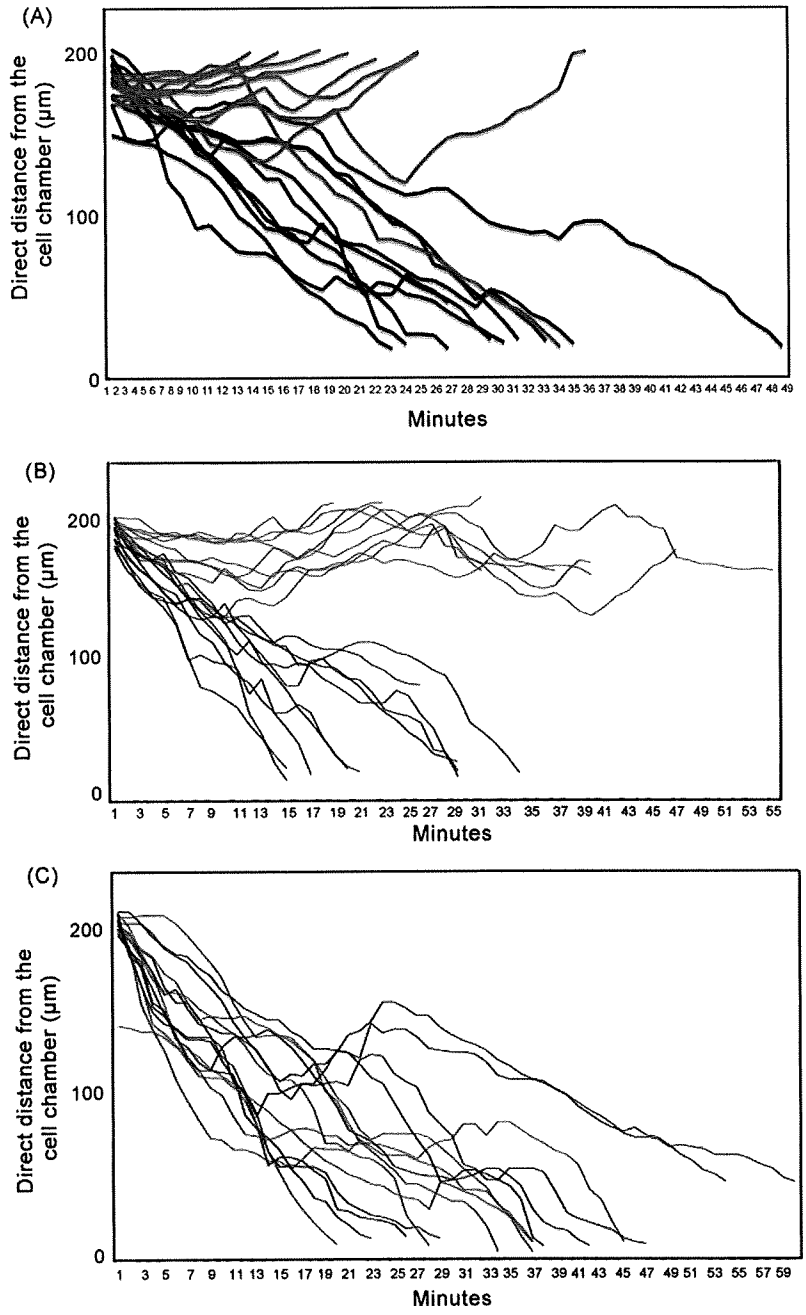

Fig. 3. Chemotaxis assay of RXM-treated T cells by TAXIScan™. Ten randomly selected cells were traced and the direct distances from the cell chamber measured at each time-point were plotted. Black and red lines indicate non-treated and RXM-treated Th1 (A), Th2 (B), and Treg (C) cells, respectively. The *x*-axis indicates minutes after starting chemotaxis. The *y*-axis indicates the direct distance from the cell chamber.

4. Discussion

Our study clearly showed that RXM down-regulated migration of Th1 and Th2 cells, but not Treg cells, toward corresponding chemokines without influencing chemokine receptor expression. These inhibiting effect are only found in RXM but CAM and EM. CAM and EM also have some immunomodulatory effects, the reason of the differences has been uncertain in this study. So far, there has been no clear data of CAM and EM on T cell chemotaxis. Of coarse this study used only one concentration of RXM, Kobayashi et al. reported that RXM at 1 or 10 μM significantly suppressed the production/expression of Th2 chemokines MDC and TARC in these keratinocytes [14]. In addition, the IL-2-enhanced expression level of Th2 chemokine receptor CCR4 was decreased by RXM at 10 μM [14]. Therefore, 10 μM RXM can be compared to the study. In the absence of RXM-pretreatment, Th1 cells migrated to IP-10, and Th2 cells to TARC. These events were associated with an increase in Ca^{++} influx and F-actin polymerization. Interestingly, our results indicate that RXM itself down-regulate F-actin polymerization in Th1 and Th2 but in Treg cells. Furthermore, chemokine-induced migration was down-regulated in RXM-pretreated Th1 and Th2 cells. In these cells, Ca^{++} influx was not as intense and F-actin polymerization was not as remarkable compared to cells without RXM pre-treatment upon incubation with corresponding chemokines. So far, there has been no report showing the effect of RXM on Ca^{++} concentration and actin polymerization in T cells. Thus, we can only speculate that RXM mainly affects the intracellular signaling pathways that lead to chemokine-induced

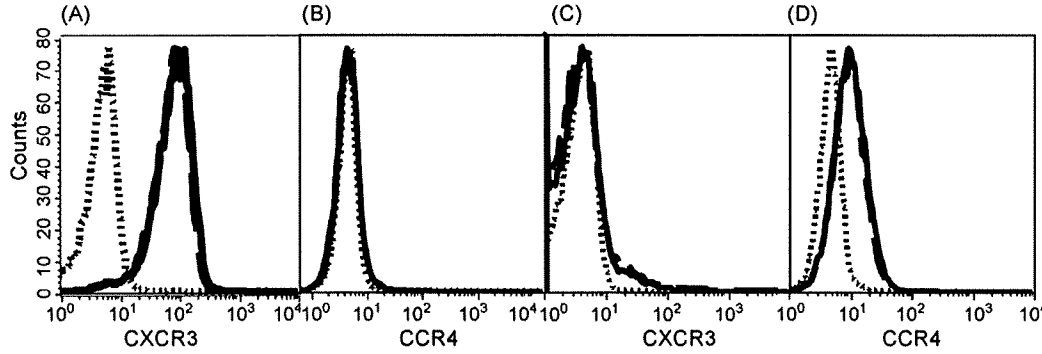

Fig. 4. Expression of CXCR3 and CCR4 on Th1, Th2, and Treg cells. (A and B) CXCR3 and CCR4 expression on Th1 cells, respectively. (C and D) CXCR3 and CCR4 expression on Th2 cells, respectively. The *x*-axis and *y*-axis indicate cell number and MFI, respectively. (—) Isotype control; (- - -) intensity of non-treated cells; (▬▬) intensity of RXM treated cells.

chemotaxis. Kobayashi et al. reported that RXM may down-regulate chemokine receptor expression on Th2 cells derived from patients with mycosis fungoides [14]. The different effect of RXM on chemokine receptor expression may come from the different cell origin, i.e., our T cells were established from normal human PBMC, and Kobayashi's from cutaneous lymphoma cells.

We do not know why RXM did not change the migration pattern in Treg cells. Chemotaxis in Treg cells has been studied in various

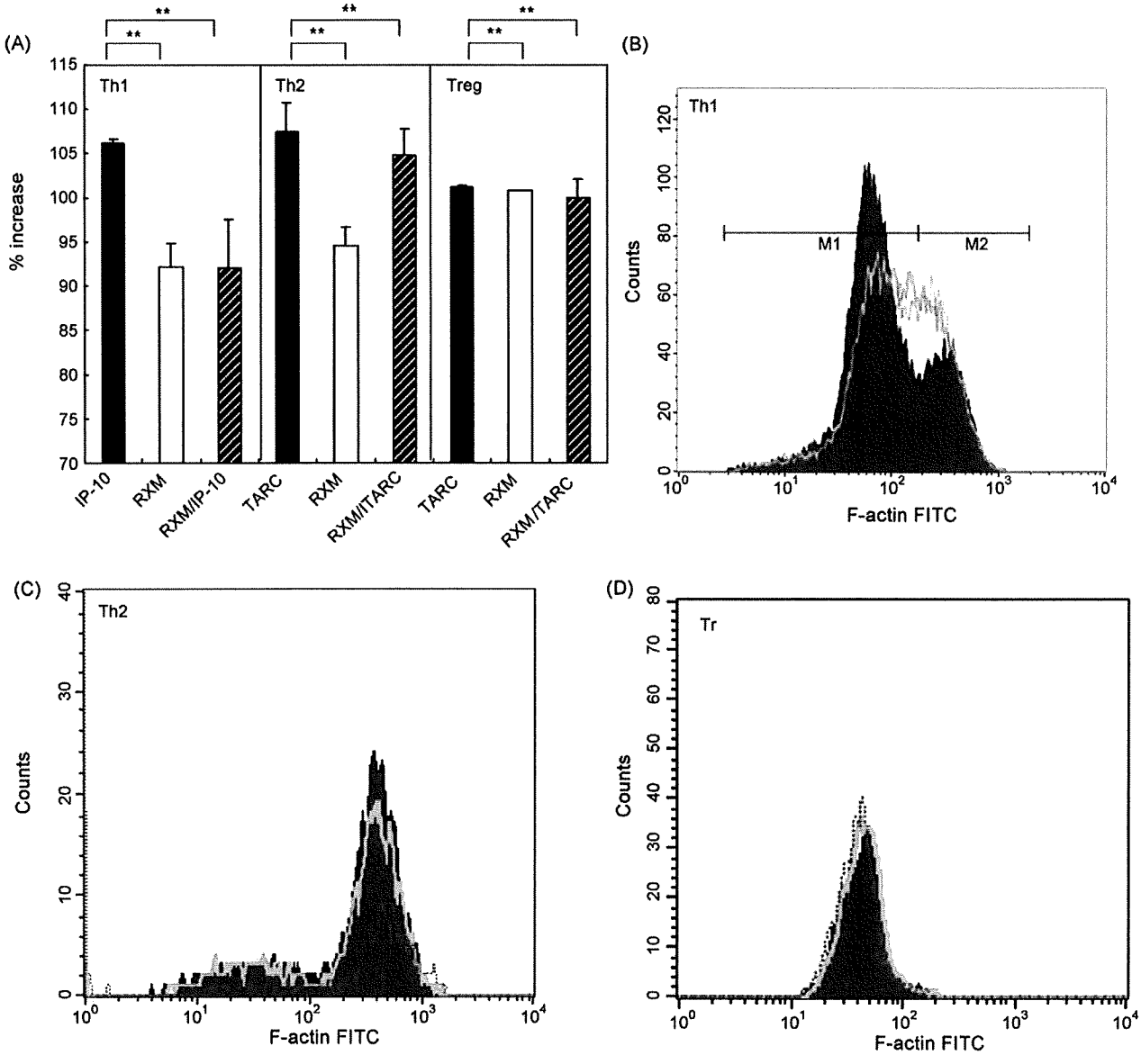

Fig. 5. F-actin polymerization assay in response to chemokines in Th1, Th2, and Treg cells. F-actin polymerization is expressed as % change compared to the baseline Ca^{++} influx in Th1, Th2, and Treg cells. (■) Ca^{++} influx induced with chemokines in untreated cells. (□) Ca^{++} influx induced with chemokines in RXM-pretreated cells. (▨) Ca^{++} influx induced with chemokines in RXM-pretreated cells. (B and C) The representative data of F-actin polymerization assay.

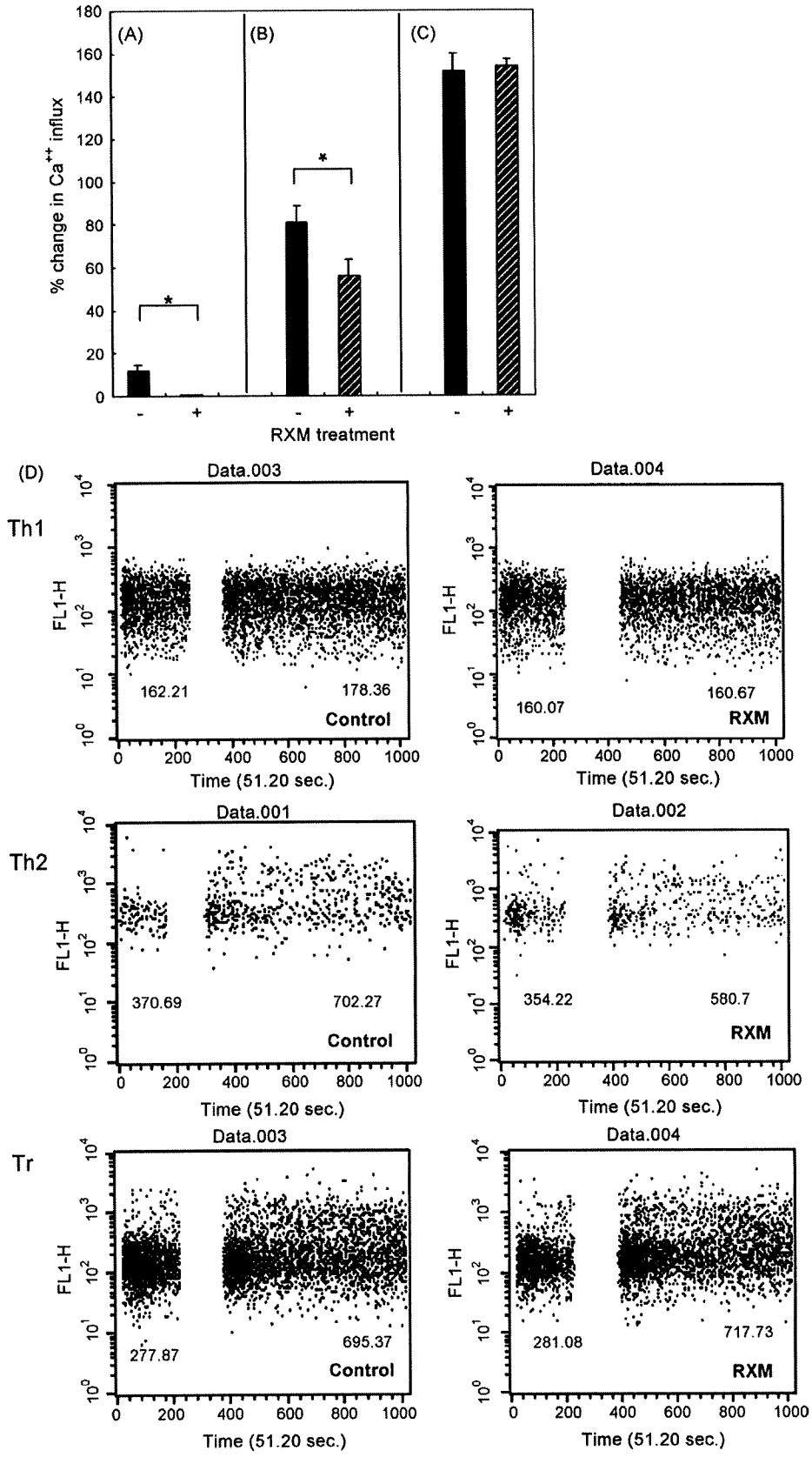

Fig. 6. (A–C) Ca^{++} influx in response to chemokines in Th1, Th2, and Treg cells. The *y*-axis indicates the % increase of MFI upon culture with chemokines (A: IP-10, B and C: TARC) compared to MFI without chemokine stimulation in Th1 (A), Th2 (B), and Treg (C) cells. (D) The representative data of Ca^{++} influx in Th1, Th2, and Treg cells.

diseases. The migratory capacity of Treg cells decreases in patients with SLE [23]. On the other hand, an increased migratory capacity of Treg cells is one of the reasons for impaired anti-tumor immunity in patients with cancer [24]. Thus, the altered migratory profiles may contribute to defective protective immunity, which underlies the pathogenesis of these disorders.

Cell migration is controlled by the formation of lamellipodia and filopodia at the leading edge [25–27]. To form these structures, actin polymerization has to occur in the leading edge in association with the redistribution of integrins, chemokine receptors, and signaling molecules [28]. Not only the activating processes, but also inactivating signals of deploymerization are important for chemotaxis [29–31]. RXM may affect some molecules in the chemotaxis cascade or Ca^{++} channels on Th1 and Th2 cells without changing chemokine receptor expression. Our study suggests that RXM exerts an immunomodulatory effect on both of Th1 and Th2 diseases through influencing chemotaxis of Th1 and Th2 cells. Lack of the RXM effect in Treg cells may also be critical in immunomodulation.

References

[1] Epstein ME, Amodio-Groton M, Sadick NS. Antimicrobial agents for the dermatologist. II: Macrolides, fluoroquinolones, rifamycins, tetracyclines, trimethoprim-sulfamethoxazole, and clindamycin. J Am Acad Dermatol 1997; 37:365–81.

[2] Bell SC, Senini SL, McCormack JG. Macrolides in cystic fibrosis. Chronic Resp Dis 2005;2:85–98.

[3] Takahashi H, Suzuki Y, Miyauchi Y, Hashimoto Y, Ishida-Yamamoto A, Iizuka H. Roxithromycin decreases ultraviolet B irradiation-induced reactive oxygen intermediates production and apoptosis of keratinocytes. J Dermatol Sci 2004; 34:25–33.

[4] Asano K, Kamakazu K, Hisamitsu T, Suzaki H. Modulation of Th2 type cytokine production from human peripheral blood leukocytes by a macrolide antibiotic, roxithromycin, in vitro. Int Immunopharmacol 2001;1:1913–21.

[5] Konno S, Adachi M, Asano K, Okamoto K, Takahashi T. Anti-allergic activity of roxithromycin: inhibition of interleukin-5 production from mouse T lymphocytes. Life Sci 1993;52:25–30.

[6] Urasaki Y, Nori M, Iwata S, Sasaki T, Hosono O, Kawasaki H, et al. Roxithromycin specifically inhibits development of collagen induced arthritis and production of proinflammatory cytokines by human T cells and macrophages. J Rheumatol 2005;32:1765–74.

[7] Wakita H, Tokura Y, Furukawa F, Takigawa M. The macrolide antibiotic, roxithromycin suppresses IFN-gamma-mediated immunological functions of cultured normal human keratinocytes. Biol Pharm Bull 1996;19:224–7.

[8] Ohshima A, Takigawa M, Tokura Y. CD8+ cell changes in psoriasis associated with roxithromycin-induced clinical improvement. Eur J Dermatol 2001;11: 410–5.

[9] Komine M, Tamaki K. An open trial of oral macrolide treatment for psoriasis vulgaris. J Dermatol 2000;27:508–12.

[10] Komiya N, Tamaoki K. Therapeutic effects of macrolides on patients with psoriasis vulgaris, pigmentary prurigo, or eosinophilic pustule folliculitis. Jpn J Antibiot 2001;54(Suppl. A):100–2.

[11] Aggarwal BB, Shishodia S, Sandur SK, Pandey MK, Sethi G. Inflammation and cancer: how hot is the link? Biochem Pharmacol 2006;72:1605–21.

[12] Sallusto F, Lenig D, Mackay CR, Lanzavecchia A. Flexible programs of chemokine receptor expression on human polarized T helper 1 and 2 lymphocytes. J Exp Med 1998;187:875–83.

[13] Komine Mayumi, Kakinuma Takashi, Kagami Shinji, Hanakawa Yasushi, Hashimoto Koji, Tamaki Kunihiko. Mechanism of thymus- and activation-regulated chemokine (TARC)/CCL17 production and its modulation by roxithromycin. J Invest Dermatol 2005;125:491–8.

[14] Kobayashi M, Shimauchi T, Hino R, Tokura Y. Roxithromycin downmodulates Th2 chemokine production by keratinocytes and chemokine receptor expression on Th2 cells: its dual inhibitory effects on the ligands and the receptors. Cell Immunol 2004;228:27–33.

[15] Santangelo S, Cousins DJ, Winkelmann NE, Staynov DZ. DNA methylation changes at human Th2 cytokine genes coincide with DNase I hypersensitive site formation during CD4(+) T cell differentiation. J Immunol 2002;169:1893–903.

[16] McHugh SM, Rifkin IR, Deighton J, Wilson AB, Lachmann PJ, Lockwood CM, et al. The immunosuppressive drug thalidomide induces T helper cell type 2 (Th2) and concomitantly inhibits Th1 cytokine production in mitogen- and antigen-stimulated human peripheral blood mononuclear cell cultures. Clin Exp Immunol 1995;99:160–7.

[17] Zheng SG, Gray JD, Ohtsuka K, Yamagiwa S, Horwitz DA. Generation ex vivo of TGF-beta-producing regulatory T cells from CD4+CD25-precursors. J Immunol 2002;169:4183–9.

[18] Zeng R, Spolski R, Finkelstein SE, Oh S, Kovanen PE, Hinrichs CS, et al. Synergy of IL-21 and IL-15 in regulating CD8+ T cell expansion and function. J Exp Med 2005;201:139–48.

[19] Kanegasaki S, Nomura Y, Nitta N, Akiyama S, Tamatani T, Goshoh Y, et al. A novel optical assay system for the quantitative measurement of chemotaxis. J Immunol Methods 2003;282:1–11.

[20] Kao JP, Harootunian AT, Tsien RY. Photochemically generated cytosolic calcium pulses and their detection by fluo-3. J Biol Chem 1989;264:8179–84.

[21] Garcia-Vicuna R, Gomez-Gaviro MV, Dominguez-Luis MJ, Pec MK, Gonzalez-Alvaro I, Alvaro-Gracia JM, et al. CC and CXC chemokine receptors mediate migration, proliferation, and matrix metalloproteinase production by fibroblast-like synoviocytes from rheumatoid arthritis patients. Arthritis Rheum 2004;50:3866–77.

[22] Cooper JA. Effects of cytochalasin and phalloidin on actin. J Cell Biol 1987;105:1473–8.

[23] Lee HY, Hong YK, Yun HJ, Kim YM, Kim JR, Yoo WH. Altered frequency and migration capacity of CD4+CD25+ regulatory T cells in systemic lupus erythematosus. Rheumatology (Oxford) 2008;47:789–94.

[24] Mizukami Y, Kono K, Kawaguchi Y, Akaike H, Kamimura K, Sugai H, et al. CCL17 and CCL22 chemokines within tumor microenvironment are related to accumulation of Foxp3+ regulatory T cells in gastric cancer. Int J Cancer 2008;122: 2286–93.

[25] Caterina MJ, Devreotes PN. Molecular insights into eukaryotic chemotaxis. FASEB J 1991;15:3078–85.

[26] Bailly M, Jones GE. Polarised migration: cofilin holds the front. Curr Biol 2003; 13:R128–30.

[27] Dawe HR, Minamide LS, Bamburg JR, CrAm LP. ADF/cofilin controls cell polarity during fibroblast migration. Curr Biol 2003;13:252–7.

[28] Arber S, Barbayannis FA, Hanser H, Schneider C, Stanyon CA, Bernard O, et al. Regulation of actin dynamics through phosphorylation of cofilin by LIM-kinase. Nature 1998;393:805–9.

[29] Sanchez-Madrid F, del Pozo MA. Leukocyte polarization in cell migration and immune interactions. EMBO J 1999;18:501–11.

[30] Yang N, Higuchi O, Ohashi K, Nagata K, Wada A, Kangawa K, et al. Cofilin phosphorylation by LIM-kinase 1 and its role in Rac-mediated actin reorganization. Nature 1998;393:809–12.

[31] Toshima J, Toshima JY, Amano T, Yang N, Narumiya S, Mizuno K. Cofilin phosphorylation by testicular protein kinase 1 and its role in integrin-mediated actin reorganization and focal adhesion formation. Mol Biol Cell 2001;12:1131–45.

Correspondence

Emergence of circulating monomyeloid precursors predicts reactivation of human herpesvirus-6 in drug-induced hypersensitivity syndrome

DOI: 10.1111/j.1365-2133.2009.09280.x

Sir, Drug-induced hypersensitivity syndrome (DIHS) is a severe cutaneous adverse event characterized by lymphadenopathy, fever, skin rashes, atypical lymphocytosis, blood eosinophilia and multiple organ dysfunctions.[1] Recent observations have reinforced the idea of transient reactivation of human herpesvirus (HHV)-6 and/or cytomegalovirus (CMV) during the disease course, which sometimes has a severe impact on the disease course and can even cause life-threatening complications.[2] We found a transient increase of a distinct subset of circulating monomyeloid precursors containing cytoplasmic HHV-6 antigens in patients with DIHS during the early phase.

Ten patients with DIHS (four men and six women; mean ± SD age 52·2 ± 20·8 years, range 18–82) on the basis of the previously proposed criteria[1] were enrolled in this study. The culprit drugs of these cases were carbamazepine (five cases), zonisamide (two cases), phenobarbital (one case), tribenoside (one case) and allopurinol (one case), and the mean ± SD interval between drug intake and onset was 49·6 ± 47·1 days (range 17–180). In all cases one or more HHV reactivations had been serologically confirmed. In two cases we could not find HHV-6 reactivation during the disease

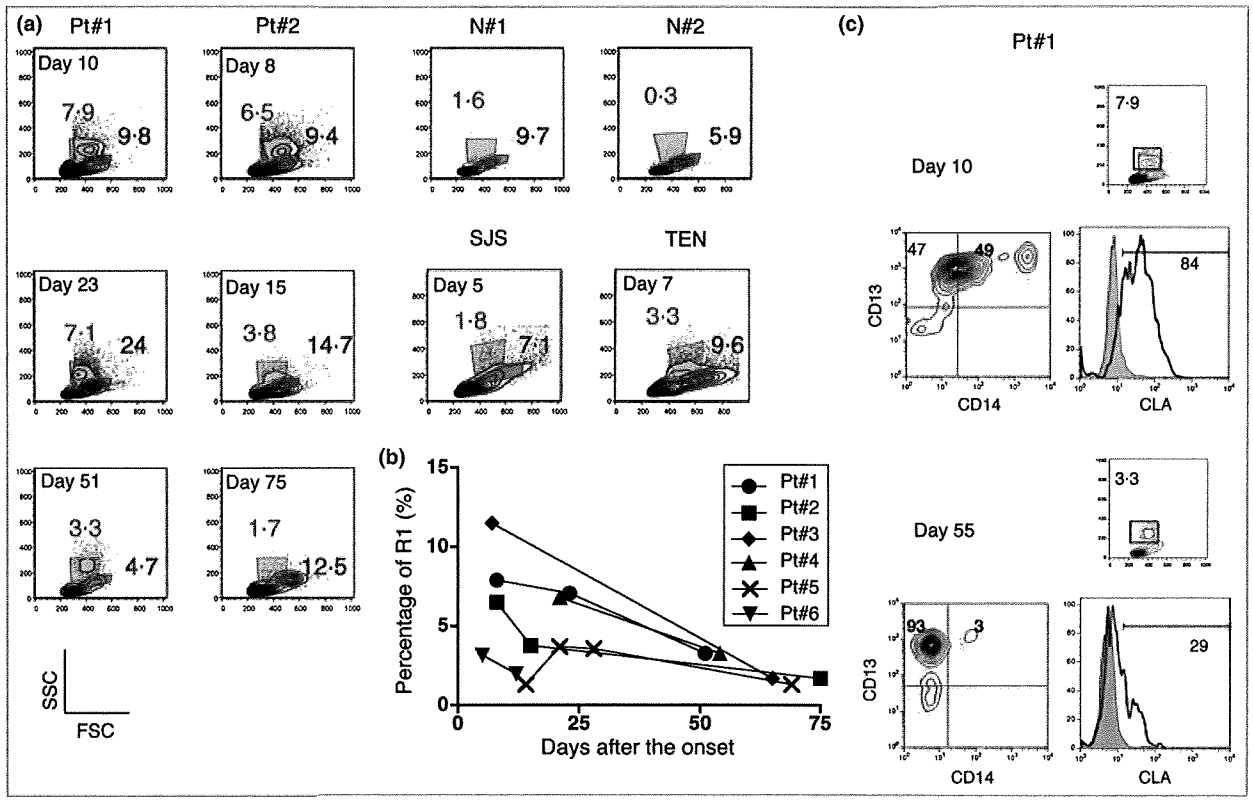

Fig 1. Emergence of monomyeloid precursors in patients with drug-induced hypersensitivity syndrome (DIHS). (a) Flow cytometric analysis of peripheral blood mononuclear cells from two representative patients with DIHS (Pt#1 and Pt#2), patients with Stevens–Johnson syndrome (SJS) and toxic epidermal necrolysis (TEN), and normal individuals (N#1 and N#2). The days after disease onset are indicated for the patients. Numbers indicate the percentages of cells gated on R1 (red) and Rm (blue). *x*-Axis, forward scatter (FSC) level; *y*-axis, side scatter (SSC) level. (b) Percentages of the R1 population at different time points in patients with DIHS. (c) CD13, CD14 and CLA expression in the R1 population at day 10 and day 55 after disease onset in a representative patient. Fluorescence-activated cell sorting analysis was performed after gating of the R1 region indicated by the box. Numbers indicate the percentages of the gated populations.

course. Five patients with other drug allergies diagnosed on the basis of their clinical and pathological features, including maculopapular rash (two men, 25 and 42 years), Stevens–Johnson syndrome (one man, 52 years; one woman, 72 years) and toxic epidermal necrolysis (one woman, 27 years) as disease controls and three normal individuals (three men, 39, 40 and 46 years) as healthy controls were also investigated. Written informed consent was obtained from all subjects prior to participation in this study.

We observed by flow cytometric (FCM) analysis a cluster of cells among peripheral blood mononuclear cells (PBMC) showing high side scatter (SSC) levels [175–300 in SSC, R1 (red) in Fig. 1a] compared with normal lymphocyte and monocyte populations [75–150 in SSC, Rm (blue) in Fig. 1a] in all the patients with DIHS (representative data are shown as Pt#1 and Pt#2 in Fig. 1a). The R1 population was not observed in normal subjects (N#1 and N#2 in Fig. 1a) and showed an ambiguous cluster comprising < 4% of the PBMC in the groups other than the DIHS group (Fig. 1a). Although the size of the R1 population was highly diverse among the patients, it was 6·9 ± 2·1% (mean ± SD; range 4·1–11·3%) of the PBMC at < 10 days after disease onset, and thereafter gradually decreased to < 3% of the total cells after disease resolution in most cases of DIHS (Fig. 1b). The R1 population during the early phase was largely positive for CD11b, CD13 and CD45, but negative for CD3, CD19 and CD20, indicating a monomyeloid origin. CD14+ and CLA+ cells were 10–50% and > 45% of the R1 population at < 10 days after disease onset and decreased to < 10% and < 30% at > 18 days, respectively, although CD13 expression was constantly high as 60–90% (Fig. 1c).

As monomyeloid precursors in the bone marrow represent a major reservoir for several types of HHV in addition to secondary lymphoid tissues and glands,[3,4] we next performed FCM analyses with anti-HHV-6 A and B variants monoclonal antibody (clone 7C7 45/15; Argene SA, Varilhes, France) to detect the viral antigens in PBMC from the patients with DIHS at various time points. Recent findings have suggested that CD13 may appear on lymphocytes under certain inflammatory conditions,[5] and thus we followed the CD14+ subset as monomyeloid precursors that emerged in DIHS. While it was not detected in the three normal individuals (N#1 and N#2 in Fig. 2a) or in CD3+ cells (left column for each patient in Fig. 2a) from patients with DIHS, the viral antigen was found in CD14+ cells between 8 and 30 days in most cases (Pt#7 and Pt#10 in Fig. 2a,b), but not in a case without HHV-6 reactivation (Pt#3 in Fig. 2a,b). It was no longer detected beyond 75 days after disease onset. More than 60% of cases of DIHS have shown reactivation of HHV-6[6,7] and/or CMV[8] which can rarely be seen in the absence of severe immune suppressive conditions, suggesting a specific contribution of HHV reactivation to the pathogenesis of DIHS. Considering that about half of the cells in the emerging population expressed CLA in DIHS, these cells may enter the skin at sites of inflammatory cell infiltration and modify skin inflammation.

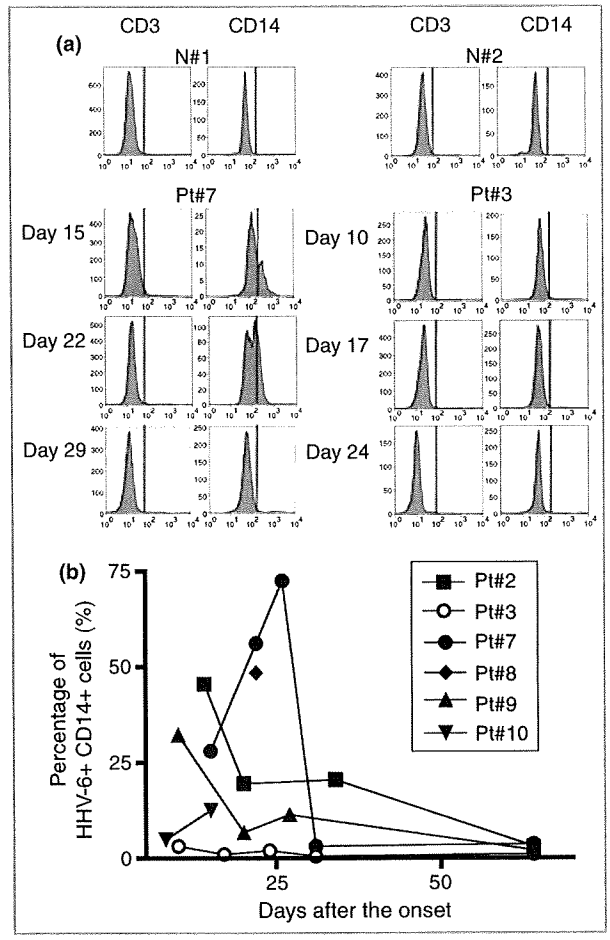

Fig 2. Detection of human herpesvirus (HHV)-6 antigens in peripheral blood mononuclear cells. (a) HHV-6 antigen-positive cells in CD3+ and CD14+ cells from two representative patients with drug-induced hypersensitivity syndrome (DIHS) (Pt#3 and Pt#7). HHV-6 antigens were never detected in Pt#3 or normal individuals (N#1 and N#2). The days after disease onset are shown. (b) Percentages of cells positive for HHV-6 antigens at different time points for patients with DIHS.

Our previous investigation of cases of DIHS revealed that drug-specific CD4+ cells are activated as the first inflammatory response followed by antivirus immune responses via CD8+ cells,[9] linked to persistent multiple organ dysfunctions and disease progression.[10] Our present observations clearly indicate that early emergence of monomyeloid precursors in the circulation is a good predictor of HHV-6 reactivation. This phenomenon would provide clues towards uncovering HHV-6 reactivation processes and lead to new strategies for preventing life-threatening complications in DIHS.

Acknowledgment

This work was partly supported by a Grant-in-Aid for Scientific Research from the Japan Society for the Promotion of Science (17594468).

Department of Dermatology, Hamamatsu University School of Medicine, 1-20-1 Higashi-ku, Handa-yama, Hamamatsu 431-3192, Japan
E-mail: hihashiz@hama-med.ac.jp

H. HASHIZUME
M. AOSHIMA
T. ITO
N. SEO
M. TAKIGAWA
H. YAGI

References

1 Hashimoto K, Yasukawa M, Tohyama M. Human herpesvirus 6 and drug allergy. *Curr Opin Allergy Clin Immunol* 2003; **3**:255–60.
2 Shiohara T, Inaoka M, Kano Y. Drug-induced hypersensitivity syndrome (DIHS): a reaction induced by a complex interplay among herpesviruses and antiviral and antidrug immune responses. *Allergol Int* 2006; **55**:1–8.
3 Zhuravskaya T, Maciejewski JP, Netski DM *et al.* Spread of human cytomegalovirus (HCMV) after infection of human hematopoietic progenitor cells: model of HCMV latency. *Blood* 1997; **90**:2482–91.
4 Kondo K, Kaneshima H, Mocarski ES. Human cytomegalovirus latent infection of granulocyte-macrophage progenitors. *Proc Natl Acad Sci USA* 1994; **91**:11879–83.
5 Saho T, Kishida T, Hirano H *et al.* Induction of CD13 on T-lymphocytes by adhesive interaction with gingival fibroblasts. *J Dent Res* 2003; **82**:893–8.
6 Tohyama M, Hashimoto K, Yasukawa M *et al.* Association of human herpesvirus 6 reactivation with the flaring and severity of drug-induced hypersensitivity syndrome. *Br J Dermatol* 2007; **157**:934–40.
7 Kano Y, Hiraharas K, Sakuma K *et al.* Several herpesviruses can reactivate in a severe drug-induced multiorgan reaction in the same sequential order as in graft-versus-host disease. *Br J Dermatol* 2006; **155**:301–6.
8 Shiohara T, Kano Y. A complex interaction between drug allergy and viral infection. *Clin Rev Allergy Immunol* 2007; **33**:124–33.
9 Hashizume H, Takigawa M. Drug-induced hypersensitivity syndrome associated with cytomegalovirus reactivation: immunological characterization of pathogenic T cells. *Acta Derm Venereol (Stockh)* 2005; **85**:47–50.
10 Hashizume H, Takigawa M, Tokura Y. Characterization of drug-specific T cells in phenobarbital-induced eruption. *J Immunol* 2002; **168**:5359–68.

Key words: CD14, *cutaneous lymphocyte-associated antigen, drug-induced hypersensitivity syndrome, human herpesvirus-6, monomyeloid lineage*

Conflicts of interest: none declared.

ORIGINAL ARTICLE

IL-10-Producing Langerhans Cells and Regulatory T Cells Are Responsible for Depressed Contact Hypersensitivity in Grafted Skin

Ryutaro Yoshiki[1], Kenji Kabashima[1], Kazunari Sugita[1], Kenji Atarashi[1], Takatoshi Shimauchi[1] and Yoshiki Tokura[1]

Although skin grafting is a common surgical technique, the immunological state of grafted skin remains unelucidated. An experimental model has shown that the development of murine contact hypersensitivity (CHS) is depressed when mice are sensitized with a hapten through full-thickness grafted skin. We explored the immunological mechanisms underlying this hyposensitization, focusing on the fate of Langerhans cells (LCs). When FITC was applied to grafted skin, FITC-bearing LCs were capable of migrating to the draining lymph nodes. Epidermal cell suspensions isolated from the grafted skin produced a high amount of IL-10 as assessed by real-time PCR. Adoptive transfer of immune lymph node cells from the sensitized mice suppressed the CHS response of recipients in an antigen-specific manner. $CD4^+CD25^+$ but not $CD4^+CD25^-$ T cells purified from lymph node cells were responsible for this suppression. Finally, we detected high expression of receptor activators of nuclear factor κ-B ligand (RANKL) in the grafted skin, and found that recombinant RANKL stimulated LCs to produce IL-10. These findings suggest that the hyposensitization of CHS through the grafted skin is not attributable merely to the reduction of LC number but that IL-10-producing LCs exert a downmodulatory effect by inducing regulatory T cells.

Journal of Investigative Dermatology (2009) **129,** 705–713; doi:10.1038/jid.2008.304; published online 9 October 2008

INTRODUCTION

Skin grafting is frequently employed in dermatology and plastic surgery. Skin grafts from the same individual can be successfully implemented 7 days after an operation, and they survive throughout the patient's life. Full-thickness skin grafts exhibit a well-matched appearance, whereas thin-thickness grafts match poorly in texture. Although there have been many cosmetic studies on skin grafting, little is known about the immunological state or the fate of immunocompetent cells in grafted skin. In particular, the function of Langerhans cells (LCs) in grafted skin is poorly understood. Clinical observations have suggested impaired immunity in grafted skin (Doiurnon *et al.*, 2001), and the lack of dermatitis on the graft is empirically known; therefore, some immunological alterations are thought to take place in the graft. Only one study has demonstrated that murine contact hypersensitivity (CHS) to a hapten cannot develop upon sensitization through full-thickness grafted skin (Yasuda *et al.*, 1996).

LCs are the major immunocompetent cells in the skin (Katz *et al.*, 1979; Stingl *et al.*, 1980) and have a positive (Silberberg-Sinakin and Thorbecke, 1980) or, in certain conditions, suppressive (Kaplan *et al.*, 2005) role in the development of CHS. They take up external antigens, migrate to draining lymph nodes, and present the antigenic determinant to naive T cells in the context of major histocompatibility complex (MHC) molecules. Thus, LCs are critical in sampling and presenting antigens in the skin. Recent studies have disclosed an immunoregulatory role of LCs. These epidermal dendritic cells (DCs) may exert a suppressive effect when they produce IL-10 (Kang *et al.*, 1998; Flacher *et al.*, 2006). This is consistent with the observation that IL-10 production by pulmonary DCs is critical for the induction of tolerance (Akbari *et al.*, 2001). Recently, it has been shown that receptor activators of nuclear factor κ-B ligand (RANKL) produced in UV light-irradiated epidermis mediate immunosuppression by modulating LCs (Loser *et al.*, 2007).

In this study, we explored the fate and functional alterations of LCs in full-thickness grafted skin using a murine CHS experimental system. Our results suggest that the immunological tolerance induced by sensitization through

[1]*Department of Dermatology, University of Occupational and Environmental Health, Kitakyushu, Japan*

Correspondence: Dr Ryutaro Yoshiki or Dr Kenji Kabashima, Department of Dermatology, University of Occupational and Environmental Health, 1-1 Iseigaoka, Yahatanishi-ku, Kitakyushu 807-8555, Japan.
E-mail: yockey@med.uoeh-u.ac.jp, kkabashi@med.uoeh-u.ac.jp

Abbreviations: CHS, contact hypersensitivity; DC, dendritic cell; dDC, dermal DC; EC, epidermal cell; LC, Langerhans cell; mAb, monoclonal antibody; MACS, magnetic cell sorting; MHC, major histocompatibility complex; PE, phycoerythrin; PCl, picryl chloride; Treg, regulatory T cell; TNF, tumor necrosis factor; RANKL, receptor activator of nuclear factor κ-B ligand

Received 30 January 2008; revised 12 July 2008; accepted 17 July 2008; published online 9 October 2008

the grafted skin is mediated by IL-10-producing LCs after the induction of $CD4^+CD25^+$ regulatory T (Treg) cells. Over-expressed RANKL in the keratinocytes of grafted skin may stimulate LCs to produce IL-10.

RESULTS

Poor development of CHS in mice sensitized with PCl through grafted skin

To confirm the previous observation by Yasuda *et al.* (1996) and to further examine whether the suppression of CHS by sensitization through skin grafting is a local or systemic phenomenon, mice were sensitized with picryl chloride (PCl) through grafted dorsal skin or non-grafted abdominal skin after skin graft implementation (on day 7 after operation). When PCl was applied to the grafted area for sensitization, the ear swelling challenge response was significantly lower than that of the positive control without skin graft (Figure 1). In contrast, sensitization of the skin-grafted mice through the non-grafted abdominal area did not abrogate CHS response. Similar data were obtained from three independent series of experiments. Thus, the depressed CHS response occurred only when sensitization was performed through the grafted local area.

Numerical alteration and apoptosis of LCs in grafted skin

LCs are critical for CHS, as they serve as antigen-presenting cells and migrate to the draining lymph nodes (Romani *et al.*, 2003). We therefore investigated the change in number of LCs in the grafted skin along with the draining lymph nodes. Epidermal sheets were taken from the grafted skin on days 7 and 14 after operation and stained with phycoerythrin (PE)-labeled anti-I-A monoclonal antibody (mAb). The number of LCs was lower in the grafted skin (200–300 mm^{-2}) on day 7 than in the untreated control skin (800–1,000 mm^{-2}). Moreover, the number of LCs in grafted skin returned to normal on day 14 (data not shown). These results indicate that the LC number was reduced at the time of sensitization. Morphologically, LCs in the grafted skin exhibited a round appearance. This reduction in LC number was not due to the migration of LCs from the skin, as the number of DCs was not increased in the regional lymph nodes (data not shown). Epidermal cell (EC) suspensions from normal skin or grafted skin were assessed for apoptosis by flow cytometry. The fraction of apoptosis in LCs was demonstrated as the Annexin-V-positive propidium iodide-negative subset in the grafted skin (Figure 2a). The percentage of apoptotic LCs was significantly increased on day 1 after grafting, but returned to the baseline on day 4 (Figure 2b).

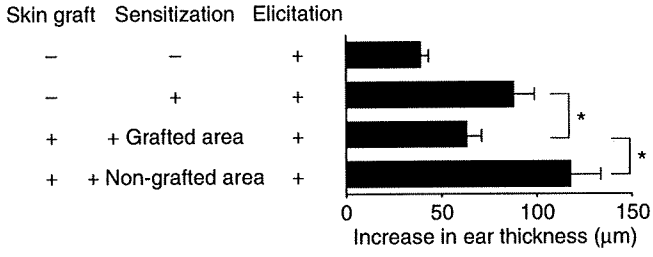

Figure 1. CHS responses in mice sensitized with PCl through grafted or non-grafted skin. Mice were sensitized with PCl on the grafted back skin or non-grafted abdominal skin 7 days after skin grafting. PCl was challenged on each earlobe 5 days after sensitization. The change in ear thickness was measured 24 hours later. Data are representative of three independent experiments. Each group consisted of more than four mice. $*P<0.05$.

Phenotypes and numbers of migrating LCs and dermal DCs in grafted skin

LCs are capable of migrating from the epidermis into the lymph nodes on sensitization (Kabashima *et al.*, 2003). The migratory ability of LCs in grafted skin was examined with FITC, which is not only a hapten but also a cell-tracking marker. On day 7 after skin grafting, FITC was applied to the grafted area. Draining lymph node cells were taken 24 hours later and labeled with allophycocyanin-labeled anti-I-A mAb, anti-mouse CD205 rat IgG, followed by PE-conjugated anti-rat IgG mAb. $FITC^+$ MHC class II^+ cells were defined as migrating DCs from the skin. CD205 is expressed by LCs as well as by dermal DCs (dDC; Henri *et al.*, 2001). In fact,

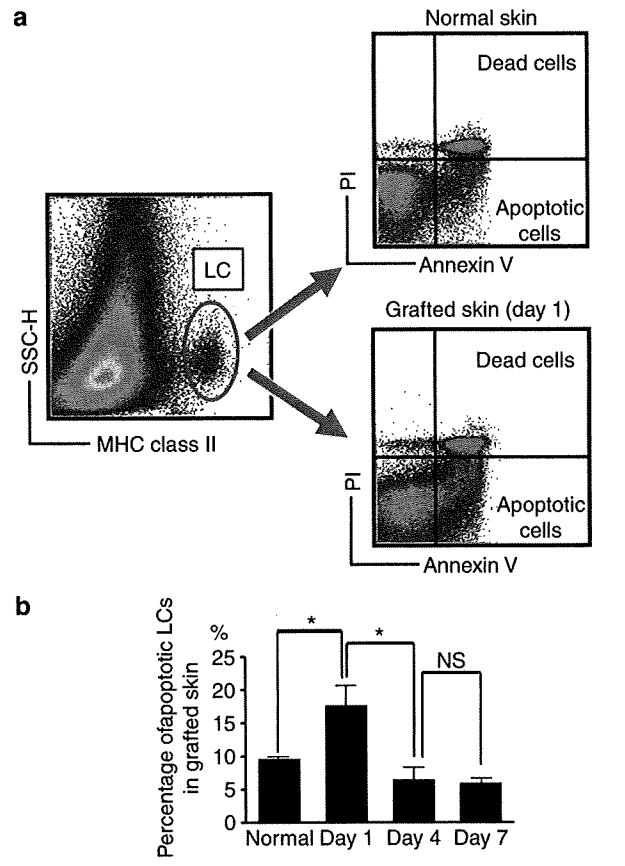

Figure 2. Numerical and morphological alterations and apoptosis of LCs in grafted skin. (**a**) Apoptosis of Langerhans cells in the grafted skin. EC suspensions from the 1-day grafted or non-grafted skin were stained with FITC-conjugated MHC class II, APC-conjugated Annexin V and PI. Apoptotic LCs were defined as MHC class II^+ Annexin V^+, but PI^-, whereas necrotic cells were double positive. (**b**) Percentage of apoptotic LCs after grafting procedure. Day 0 represents normal skin and day 1, 4, or 7 shows the day after grafting. Data are representative of three independent experiments. Each group consisted of five mice. $*P<0.05$.

migrating DCs were divided into a CD205$^+$ Langerin$^+$ subset and a CD205$^-$ Langerin$^-$ subset. Therefore, the vast majority of FITC$^+$ MHC class II^{hi} CD205$^+$ cells represent LCs, whereas FITC$^+$ MHC class II^{hi} CD205$^-$ cells are mostly dDCs (Figure 3a).

To determine whether migrating LCs/dDCs in grafted skin retained their antigen-presenting capacity, migrating DCs were stained with PE-conjugated mAbs to CD80 and CD86. CD80 and CD86 were present on both LCs and dDCs. Thus, LCs/dDCs in grafted skin retained their antigen-presenting capacity for naive T cells.

Compared to the control mice painted with FITC on normal skin, the mice sensitized at the skin-grafted site had reduced numbers of both FITC$^+$ MHC class II^{hi} CD205$^+$ and FITC$^+$ MHC class II^{hi} CD205$^-$ populations in the draining lymph nodes (Figure 3c). From three independent series of experiments, the number of LCs and/or DCs in the lymph nodes of grafted skin–sensitized mice was approximately one-fourth that of normal skin–sensitized mice (Figure 3c). Considering that the grafted skin originally had about one-fourth the LCs of normal skin, the migratory ability of LCs in grafted skin was virtually the same as that in normal skin.

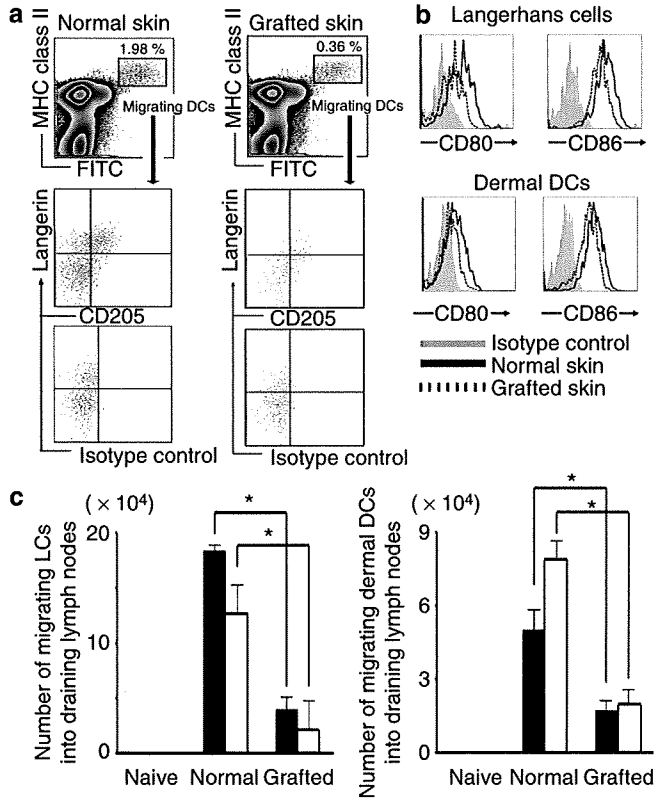

Figure 3. Expression of co-stimulatory molecules and number of migrating DCs in grafted mice. (**a**) Draining lymph node cells were taken from mice painted with FITC on the grafted or normal skin and stained with anti-MHC class II, CD205 and Langerin mAbs. CD205$^+$ cells are virtually the same population as Langerin$^+$ cells. (**b**) After being stained with anti-CD205, CD80, and CD86 mAbs, lymph node cells were subjected to flow cytometric analysis to assess the expression of co-stimulatory molecules. (**c**) Numbers of FITC$^+$ MHC class II^{hi} CD205$^+$ cells (mainly LCs) and FITC$^+$ MHC class II^{hi} CD205$^-$ cells (mainly dDCs) migrating from the skin to the draining lymph nodes. The numbers are calculated based on flow cytometric analysis gated as seen in Figure 3a. Each group consisted of more than four mice. *$P<0.05$.

Increased IL-10 expression in grafted skin

It is well known that UV B (UVB) radiation has immunosuppressive effects on normal cutaneous processes (Elmets *et al.*, 1983; Yagi *et al.*, 1996) and this UV-induced immunosuppression is associated with upregulation of anti-inflammatory Th2 cytokines, IL-4 and IL-10 (Rivas and Ullrich, 1992; Shreedhar *et al.*, 1998). Among cytokines, IL-10 is critical for CHS suppression (Simkin *et al.*, 2000), and both LCs (Takashima, 1995; Flacher *et al.*, 2006) and keratinocytes (Rivas and Ullrich, 1992) are possible candidates for the IL-10 source. To address the involvement of IL-10, mice receiving skin grafts (day 0) were either sensitized with PCl (day 7) on the dorsal grafted skin or untreated. As control, mice without skin grafts were sensitized with PCl on the dorsal skin or untreated. EC suspensions were obtained from the dorsal skin of these four experimental groups (day 8). As shown in Figure 4a, whereas the normal skin had little or no ability to elaborate IL-10 irrespective of PCl sensitization, the grafted skin expressed high levels of IL-10 mRNA, as assessed by real-time PCR. Relative amounts of mRNA were measured by the $\Delta\Delta C_t$ method (Atarashi *et al.*, 2007). Although both grafted skin samples with and without subsequent PCl painting yielded IL-10 mRNA, the nonsensitized epidermis was more productive; it may be that IL-10 produced by keratinocytes was reduced in proportion to

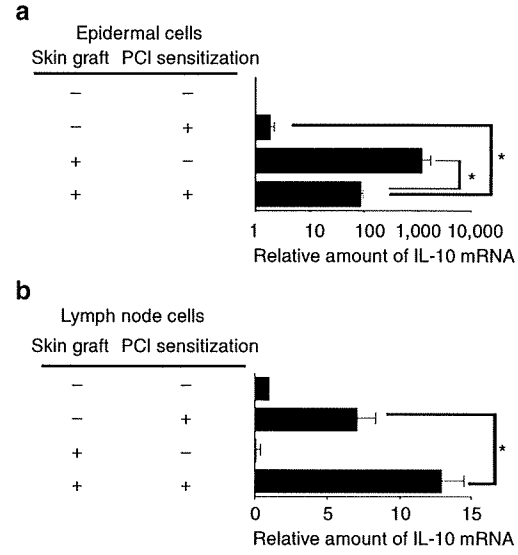

Figure 4. IL-10 expression in ECs and lymph node cells from grafted mice. (**a**) Epidermal sheets were prepared from grafted (7 days after operation) or non-grafted skin that was painted with PCl or left untreated. IL-10 mRNA expression was measured by real-time PCR. (**b**) Draining lymph node cells were obtained 5 days after sensitization of mice through grafted or non-grafted skin. IL-10 mRNA expression was measured by real-time PCR. The relative amounts of mRNA expression were calculated using the $\Delta\Delta C_t$ method. Each group consisted of more than four mice. Data are the mean ± SD of three independent experiments. *$P<0.05$.

PCI sensitization or, alternatively, IL-10-producing LCs emigrated on sensitization.

Along with ECs, we examined the expression of IL-10 mRNA in the draining lymph nodes. Lymph node cells were prepared from mice receiving skin grafts and/or subsequent PCI painting. Skin grafting alone did not augment IL-10 production by lymph node cells (Figure 4b). PCI sensitization on the grafted skin dramatically enhanced the production of IL-10. This increase of IL-10 was considered to be derived from LCs or proliferative T cells in the draining lymph nodes. As the PCI-painted grafted skin produced less IL-10 than the PCI-non-painted grafted skin (see Figure 3a), we postulate that IL-10-producing LCs emigrated from the grafted skin to the lymph nodes on sensitization with PCI.

LCs as a source of IL-10 in grafted skin

To dissect the cytokine-producing populations in grafted skin, EC and dermal cell suspensions were prepared from grafted (day 7) or normal skin. EC suspensions and dermal cell suspensions were fractionated to $CD11c^+$ (containing 70–80% LCs or dDCs and <0.01% T cells) and $CD11c^-$ (containing mainly keratinocytes or fibroblasts and <0.05% DCs) subsets with magnetic cell sorting (MACS). As shown in Figure 5, both $CD11c^+$ and $CD11c^-$ fractions produced a high amount of IL-10, indicating that not only keratinocytes but also LCs from the grafted skin were stimulated to produce IL-10. In contrast, $CD11c^-$ cells secreted more IL-6 in grafted skin than normal skin, suggesting that keratinocytes in the graft produced IL-6. Both $CD11c^+$ and $CD11c^-$ cells produced higher amounts of tumor necrosis factor-α (TNF-α) in the grafted skin than in the normal skin. Surgical trauma induces an early hyperinflammatory response, which is characterized by proinflammatory TNF-α, IL-1, and IL-6 cytokine release (Menger and Vollmar, 2004). IL-6 has a crucial role in the neutrophil and macrophage infiltration in the wound healing process (Lin *et al.*, 2003). Thus, this increase of IL-6 and TNF-α is considered to be a hyperinflammatory response of the wound healing process.

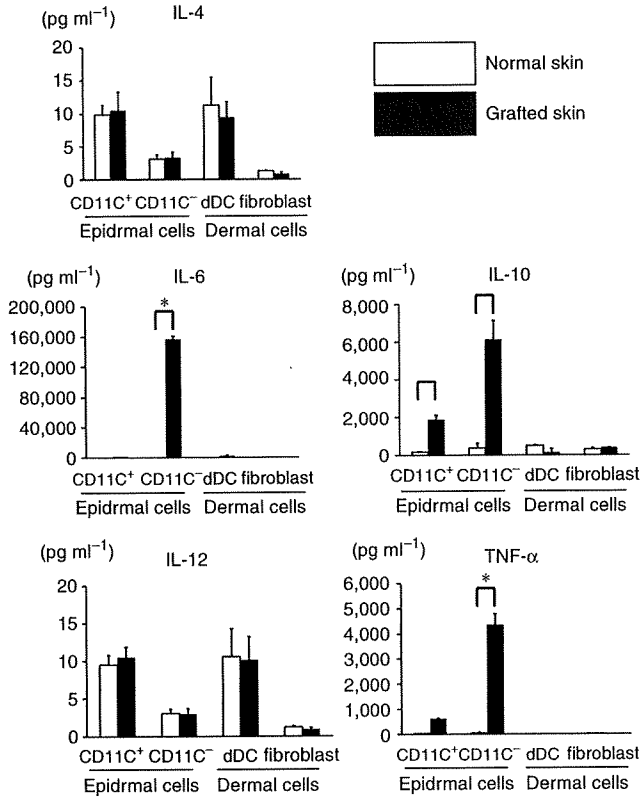

Figure 5. Cytokine production by ECs and dermal cells. EC suspensions were obtained from grafted or non-grafted skin, and fractionated to $CD11c^+$ cells (70–80% LCs) and $CD11c^-$ cells (LC-depleted cells, mainly keratinocytes) with auto-MACS using CD11c microbeads. Dermal cell suspensions were centrifuged with Ficoll-Paque, followed by auto-MACS, to fractionate dDCs and other cells (mainly fibroblasts). Each subset was cultured for 24 hours. The amounts of IL-4, IL-6, IL-10, IL-12, and TNF-α in the culture supernatants were quantified using cytometric beads array. Data are the mean ± SD of three independent experiments. Each group consisted of more than four mice. *P<0.05.

Induction of $CD4^+CD25^+$ regulatory T cells by sensitization through grafted skin

The presence of IL-10-producing LCs in the epidermis and lymph nodes raised the possibility that Treg cells were induced in mice sensitized with PCI through grafted skin. We performed an adoptive transfer study to evaluate this possibility. Donor mice were sensitized with PCI on the grafted skin, and lymph nodes and spleen cells were taken from the mice 5 days later (Figure 6, top). $CD4^+CD25^+$ and $CD4^+CD25^-$ subsets were purified from the pooled cells by

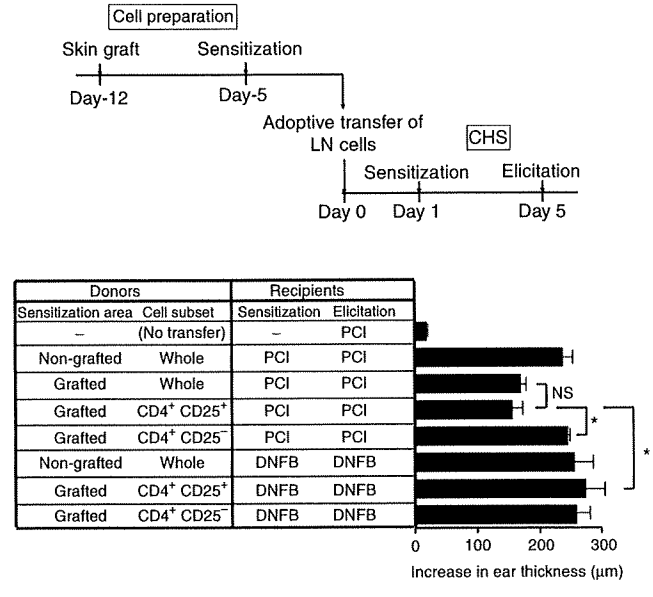

Figure 6. Transfer study of $CD4^+CD25^-$ cells from donor mice sensitized through grafted skin. Mice were sensitized with PCI on the grafted (7 days after operation) or non-grafted area. Five days after sensitization, draining lymph nodes and spleen cells were taken from the mice. Whole cells, $CD4^+CD25^+$ sorted cells, or $CD4^+CD25^-$ sorted cells were transferred into syngeneic naive mice (5×10^6 for each mouse). Then, the recipients were sensitized on the dorsum and challenged on the ears with hapten (PCI or DNFB) as indicated in the figure. Change in ear thickness was measured 24 hours later. Each group consisted of more than four mice. Data are representative of three independent experiments. *P<0.05.

MACS. Whole unfractionated cells or cells of each subset were transferred into syngeneic naive recipients (5×10^6 for each mouse), which were then sensitized and challenged with PCl. The transfer of $CD4^+CD25^+$ T cells decreased the CHS response of the recipients, whereas $CD4^+CD25^-$ T cells were not suppressive (Figure 6, bottom). When recipient mice were sensitized and challenged with another hapten dinitrofluorobenzene, such suppression was not observed, suggesting that the immunosuppression was antigen specific. Thus, the depressed sensitization through the grafted skin was associated with the appearance of $CD4^+CD25^+$ Treg cells.

Augmentation of IL-10 production by LCs exposed to RANKL

It has been recently reported that LCs express receptor activators of nuclear factor κ-B, that UVB irradiation upregulates cutaneous RANKL, and that RANKL activates DCs as well as Tregs in the skin (Loser *et al.*, 2006). We hypothesized that the grafted skin expresses RANKL and activates LCs to produce IL-10. When the grafted skin was stained with anti-RANKL and MHC class II antibodies, we found that ECs of the grafted skin expressed RANKL (Figure 7a, RANKL, blue; LCs, red). Notably, RANKL was strongly expressed around LCs (merged purple), suggesting that receptor activators of nuclear factor κ-B/RANKL interactions might be important for the induction of hyposensitization in grafted skin. To identify the function of receptor activator of nuclear factor κ-B/RANKL in the skin immune system, we tested the ability of LCs to produce IL-10 when they were exposed to recombinant RANKL. EC suspensions were cultured with or without recombinant RANKL (R&D Systems, McKinley, MN) for 24 hours, and stained with anti-MHC class II antibody. Then, the cells were permeabilized and stained with anti-IL-10 antibody. We found that the addition of RANKL increased the fraction of IL-10-positive LCs (Figure 6b) and the mean fluorescence intensity of IL-10 in LCs (Figure 6c). These findings indicated that RANKL expressed by keratinocytes of grafted skin stimulates LCs to produce IL-10.

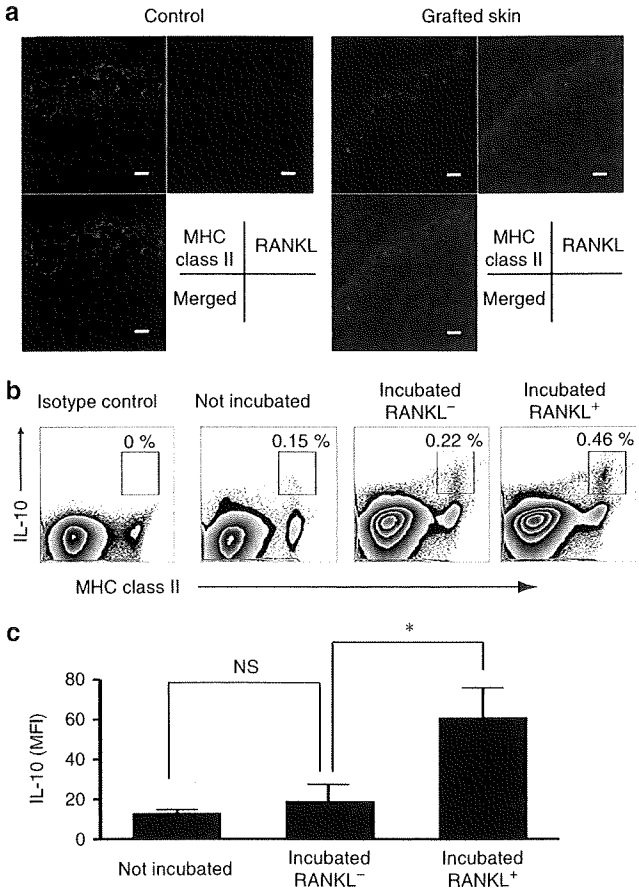

Figure 7. Induction of RANKL in grafted skin and stimulation of LCs to produce IL-10 by RANKL. (**a**) The grafted or non-grafted skin was stained with antibodies to MHC class II and RANKL. Red, MHC-class II; blue, RANKL. Merged image is shown in purple. (**b**, **c**) EC suspensions were cultured with or without recombinant RANKL for 2 days. Cells were fixed, permeabilized, stained with IL-10 and MHC class II antibodies, and analyzed by flow cytometry (**b**). The mean fluorescence intensity of IL-10 in MHC class II + LCs existing in EC suspensions. Bars indicate the mean + SD. Data are representative of three independent experiments. Each group consisted of more than four mice. Scale bar = 50 μm $^*P<0.05$.

DISCUSSION

This study addressed the immunological mechanism underlying impaired sensitization through grafted skin. CHS was depressed only when mice were immunized with hapten through grafted skin, and even skin graft-bearing mice fully developed CHS when sensitized through non-grafted skin. Therefore, the induction of immunosuppression is local, whereas its effects are specific. The local immunological condition of the grafted skin is responsible for impaired induction. The fate of LCs in the graft seems to be a key to resolving the mechanism. Mainly because of the apoptotic death of LCs, the number of LCs in freshly implemented skin was up to one-fourth that of normal skin. However, when FITC was applied to the grafted skin, FITC-bearing LCs were present in the draining lymph nodes, again at a cell number one-fourth that of normal skin–sensitized mice. Thus, LCs were capable of migrating efficiently from the grafted skin to the draining lymph nodes. As LCs can serve as both positive and negative antigen-presenting cells depending on the surrounding milieu (Silberberg-Sinakin and Thorbecke, 1980; Kaplan *et al.*, 2005), not only the numerical but also functional changes of LCs determine CHS development. We further investigated whether the hyposensitization of CHS through grafted skin was attributable merely to the reduction of LC number, or whether some function of LCs was altered.

DCs in peripheral tissues, such as epidermal LCs, remain immature in the steady state, and express small quantities of MHC class II and co-stimulatory molecules and produce low levels of immunostimulatory cytokines. During the process of antigen capture/presentation and migration into T-cell areas of regional lymph nodes, maturation of DCs simultaneously occurs, as they express high amounts of these surface molecules and cytokines (Inaba *et al.*, 1997; Huang *et al.*, 2000; Lutz and Schuler, 2002). Recent studies have revealed that peripheral tolerance is induced by immature DCs (Steinman *et al.*, 2000; Lutz and Schuler, 2002) or partially

by mature DCs that express MHC class II, CD80 and CD86 molecules but lack secretion of IL-12, IL-6, and TNF-α (Groux, 2003). On the basis of their migrating ability, it seemed that nonapoptotic, live LCs in the grafted skin were functionally mature.

Given that surgical trauma is one of the injuries that induce a hyperinflammatory response, the skin graft employed in this study likely leads to the production of proinflammatory cytokines such as TNF-α and IL-6. However, the skin graft is not merely surgical trauma, because living skin is applied to the raw surface. More specifically, the intact ECs produce high amounts of IL-6 and TNF-α (see Figure 5), suggesting that skin grafting induces inflammatory cytokine production more vigorously than simple trauma. In wound healing after skin grafting, the exaggerated inflammatory response should be downregulated in due course. Among various factors that suppress the inflammatory response, IL-10 is one of the most important candidates, because it is a potent inhibitor of the activation of monocytes/macrophages and of the expression of TNF-α and other proinflammatory mediators (Denys *et al.*, 2002). In fact, IL-10 was produced at a high level by keratinocytes in grafted skin. We explored the possibility that LCs have a polarized cytokine production pattern in the graft, which leads to peripheral tolerance. In this scenario, IL-10 is a strong candidate as a skewing cytokine.

LCs in grafted skin exhibited a rounder and less dendritic appearance than those in normal skin. Along with this morphological change, LCs in grafted skin expressed IL-10 at a higher level than those in non-grafted skin, suggesting that IL-10-producing LCs have an important role in depressed CHS. Many studies have shown that IL-10 is an essential cytokine in depression of CHS (Annacker *et al.*, 2001; Girolomoni *et al.*, 2004; Ghoreishi and Dutz, 2006). Similarly, IL-10 production by pulmonary DCs is critical for the induction of tolerance (Akbari *et al.*, 2001). Besides LCs, keratinocytes also secrete IL-10, which causes CHS suppression when overexpressed by certain stimuli such as UVB radiation (Schwarz *et al.*, 2004; Ghoreishi and Dutz, 2006). Keratinocyte-derived IL-10 might further condition LCs to be regulatory as well as suppress the injury-associated inflammation.

Conversely, the adoptive transfer of $CD4^+CD25^+$ T cells from the tolerant mice induced CHS suppression, whereas $CD4^+CD25^-$ T cells had no effect. This suggests that $CD4^+CD25^+$ Treg cells as well as IL-10-producing LCs participate in the skin graft-induced suppression of CHS. At present, at least four types of Treg cells can be identified based on the expression of cell-surface markers, secretion of cytokines, and suppression mechanisms (Groux, 2003). Recent accumulating evidence has indicated that Treg cells have a key role in peripheral tolerance (Takahashi *et al.*, 1998; Shevach, 2001; Taylor *et al.*, 2001; Thorstenson and Khoruts, 2001; Zhang *et al.*, 2001) under the influence of immature or maturing DCs (Min *et al.*, 2003; Roelofs-Haarhuis *et al.*, 2003).

The relationship between IL-10-producing LCs and Treg cells remains partly elucidated. In UVB-induced tolerance, intravenous transfer of Treg cells suppresses CHS, and this phenomenon is dependent on host-derived IL-10 (Ghoreishi and Dutz, 2006). Other groups have reported that Treg cells regulate the expansion of peripheral $CD4^+$ T cells with IL-10 (Annacker *et al.*, 2001). These findings have suggested that IL-10 is essential for Treg cells for successful downmodulation, and the source of IL-10 is a constituent of the immunological milieu, such as epithelial cells, or Treg cells *per se*. However, we found that LCs are the IL-10 producer, raising the possibility that IL-10-producing LCs are an inducer of Treg cells. In addition, IL-10 released from LCs also might inhibit effector T cells concerned with CHS.

A group of investigators have found that RANKL, which is expressed in the keratinocytes of inflamed skin, controls Treg cell numbers by activation of DCs (Loser *et al.*, 2007). In this study, we showed that both epidermal $CD11c^+$ LCs and $CD11c^-$ cells (keratinocytes) produce high amounts of representative proinflammatory cytokine TNF-α in the grafted area, which might lead to the expression of RANKL on keratinocytes. Our finding that LCs exposed to recombinant RANKL produced a high level of IL-10 suggests that RANKL from keratinocytes in the grafted skin can induce IL-10-producing LCs at the initiation stage of immunosuppression. The reduction in LC number may cause impaired sensitization, but in accordance with recent observations (Kaplan *et al.*, 2005; Kissenpfennig *et al.*, 2005), the altered function of LCs is more likely involved in the depression of CHS.

Our study is clinically relevant in two aspects. First, grafted skin provides a specialized immunological status, in which T cells do not respond well to external stimuli such as contactants, as a result of skewed function and a reduced number of LCs. In this context, contact dermatitis cannot easily develop in the grafted skin. Second, the skin graft may be used for the induction of antigen-specific peripheral tolerance by application of antigen through the grafted skin. This strategy may have great potential for controlling allergic diseases and autoimmune disorders. Further investigation of this skin graft-associated immunosuppression may develop safe and effective methodologies for tolerance induction.

MATERIALS AND METHODS

Mice

BALB/c (7- to 10-week-old) female mice were obtained from Kyudo Co. Ltd (Kumamoto, Japan). Mice were maintained on a 12-hour light/dark cycle under specific pathogen-free conditions. Protocols were approved by the Institutional Animal Care and Use Committee of the University of Occupational and Environmental Health.

Preparation of skin graft

One day before skin grafting, the back of each mouse was clipped and hairs were removed with depilatory cream (Shiseido Cosmetic Co., Tokyo, Japan). A 25×20 mm area of full-thickness back skin was resected under intraperitoneal anesthesia with ketamine and dolmicam. The same skin was grafted onto the back of each mouse. The graft was sutured and fixed with a tie-over dressing. The dressing was removed on day 7 after operation.

Contact hypersensitivity

For contact sensitization, 25 μl of PCl solution (0.5% w/v in acetone-olive oil mixed at 4:1) was painted on the grafted or non-grafted area. For elicitation, 10 μl of 0.2% PCl solution was painted on each earlobe of the PCl-sensitized mice on day 5 after sensitization. In some experiments, 50 μl of dinitrofluorobenzene (Nacalai Tesque Co., Tokyo, Japan) solution (0.5% w/v in acetone-olive oil mixed at 4:1) was painted on the abdomen, and elicited with 10 μl of 0.3% dinitrofluorobenzene solution on each earlobe 5 days after sensitization. The thickness of each ear was measured with a micrometer 24 hours after elicitation. Swelling was expressed as the increase in ear thickness.

Culture medium

RPMI 1640 (Gibco BRL Life Technology, Grand Island, NY) was supplemented with 10% heat-inactivated fetal calf serum, 2 mM L-glutamine, 5×10^{-5} M 2-mercaptoethanol, 10^{-5} M sodium pyruvate, 25 mM 4-(2-hydroxyethyl)-1-piperazineethanesulfonic acid, 1% nonessential amino acids, 100 U ml^{-1} penicillin, and 100 μg ml^{-1} streptomycin (all from Gibco BRL Life Technology).

Immunohistochemistry

For immunofluorescence analysis, epidermal sheets were separated from the dermis with 0.5 M ammonium thiocyanate, fixed in acetone for 5 minutes at −20 °C, and stained with PE-conjugated anti-I-A^d mAb (BD Biosciences, San Diego, CA). In some experiments, the back skin of mice was frozen in Tissue-Tek OCT compound 4583 (Sakura Finetechnical Co. Ltd, Tokyo, Japan). Cryostat sections (10 μm) were fixed in acetone and stained with PE-conjugated anti-I-A^d mAb, biotin-conjugated anti RANKL mAb (R&D Systems) followed by staining with allophycocyanin-Cy7 conjugated streptavidin. Images were viewed with a Zeiss confocal microscope and processed with an LSM Image Browser (Zeiss).

Preparation of EC and dermal cell suspensions, and purification for LCs and dDCs

Skin sheets were floated in 0.2% trypsin in phosphate-buffered saline (pH 7.4) for 1 hour at 37 °C as described previously (Tokura *et al.*, 1994). The epidermis was separated from the dermis with forceps in phosphate-buffered saline supplemented with 10% fetal calf serum. EC suspensions were prepared by pipetting and filtration through nylon mesh. Dermal cells were obtained from normal or grafted skin from which the epidermis had been removed. Samples were minced and incubated for 2 hours at 37 °C in RPMI 1640 (Invitrogen, Carlsbad, CA) supplemented with collagenase XI (4,830 U ml^{-1}; Sigma, Tokyo, Japan), hyaluronidase (260 U ml^{-1}; Sigma), DNase (0.1 mg ml^{-1}; ICN, Costa Mesa, CA), and 10 mM 4-(2-hydroxyethyl)-1-piperazine ethanesulfonic acid (Sigma). The obtained cells were filtered through a 40 μm filter. dDCs and other cells (mainly fibroblasts) were fractionated from the dermal cell suspensions with Ficoll-Paque (GE Healthcare UK Ltd) For enrichment of LCs and dDCs, EC suspensions and derma cell suspensions after Ficoll-Paque fractionation were purified for $CD11c^+$ and $CD11c^-$ subsets using anti-CD11c mAb and auto-MACS (Miltenyi Biotec, Gladbach, Germany). The purity of $CD11c^+$ cells was 70–80% (Supplementary information, Figure S1), containing less than 0.01% $CD3^+$ T cells as determined by flow cytometric analysis. The $CD11c^-$ cells from EC and dermal cell suspensions were mainly keratinocytes and fibroblasts, respectively, containing less than 0.05% DC subsets.

Flow cytometry

Cells were immunostained with various combinations of fluorescence-conjugated mAbs and analyzed with three-channel FACSCanto flow cytometer (BD Biosciences) and FlowJo software (Tree Star Inc, Ashland, OH). The expression of cell-surface and intracytoplasmic cytokines were analyzed using antibodies to PE-conjugated anti-CD11c, CD80, CD86 and PE-conjugated anti-rat IgG, purified anti-mouse CD205 (DEC205) rat IgG, PerCP-conjugated anti-CD45R mAbs, PE-conjugated anti-MHC class II, biotin-conjugated anti-IL-10, and PE-Cy7-conjugated streptavidin. Antibodies were purchased from e-Bioscience (San Diego, CA). All mAbs were used at 1–5 μg 10^{-6} cells, and each incubation was performed for 30 minutes at 4 °C, followed by two washes in phosphate-buffered saline supplemented with 5% fetal calf serum and 0.02% sodium azide. Viable cells were identified by 7-AAD uptake. Intracytoplasmic IL-10 was detected in permeabilized cell suspensions using BD Cytofix/Cytoperm Plus Kit (BD Biosciences).

Apoptosis analysis

EC suspensions from control or grafted (1, 4, and 7 days after) skin were stained with FITC-conjugated MHC-class II mAb for 30 minutes on ice and stained with allophycocyanin-conjugated Annexin V and propidium iodide (Invitrogen), according to the manufacturer's protocol. Apoptosis in LCs was analyzed by a FACScant using FlowJo software (Tree Star Inc) as described earlier (Goldszmid *et al.*, 2003).

Cutaneous DC migration into draining lymph nodes

Mice were painted with 200 μl of 2% FITC (Sigma-Aldrich, St Louis, MO), and axillar and inguinal lymph nodes were taken 24 hours later. Single-cell suspensions were prepared and subjected to flow cytometric analysis.

Real-time PCR

Total RNA was extracted from axillary and inguinal lymph nodes and EC suspensions with the SVTotal RNA isolation system (Promega, Madison, WI) according to the manufacturer's protocol. Murine IL-10 gene expression was quantified in a two-step reverse transcription–PCR. cDNA was reverse transcribed from total RNA samples using the TaqMan RT reagents (Applied Biosystems, Foster, CA). Target gene expression was quantified using TaqMan Gene Expression Assay (Applied Biosystems) in the ABI PRISM 7000 sequence detection system (Applied Biosystems). The probe was synthesized with VIC as the reporter dye and Tamra as the quencher dye. The forward primer, reverse primer, and TaqMan probe were purchased from Applied Biosystems. As an endogenous control for these PCR quantification studies, glyceraldehyde-3-phosphate dehydrogenase gene expression was measured using the TaqMan rodent GAPDH control reagents (Applied Biosystems). Results represented normalized IL-10 mRNA amounts relative to skin-grafted groups using the $\Delta\Delta C_t$ method.

Measurement of cytokine amounts in culture supernatants

$CD11c^+$ and $CD11c^-$ cells were purified from EC and dermal cell suspensions. Cells of each subset (2×10^6 cells per 1.5 ml well) were

cultured in medium for 24 hours in 24-well plates (Corning Glass Works, Corning, NJ). The concentration of IL-4, IL-6, IL-10, IL-12, and TNF-α in culture supernatants was measured using a cytometric beads array system (BD Biosciences) according to the manufacturer's protocol.

Purification and adoptive transfer of Treg cells

Axillary and inguinal lymph nodes were harvested from mice. They were meshed through a cell strainer into RPMI 1640 containing 2% fetal calf serum to prepare single-cell suspensions. To purify $CD4^+CD25^+$ cells or $CD4^+CD25^-$ cells, a mouse Treg isolation kit (Miltenyi Biotec) was used according to the manufacturer's protocol. Briefly, $CD4^-$ cells were depleted with the biotin-labeled antibody cocktail. Subsequently, the $CD4^+$ fractions were magnet-separated with CD25-PE mAb. The positive fraction contained $CD4^+CD25^+$ cells with more than 95% purity, and the flow-through fractions from magnet columns were used as $CD4^+CD25^-$ fraction.

Statistic analysis

All data were statistically analyzed using Student's *t*-test. A *P*-value of less than 0.05 was considered to be significant. Bar graphs were presented as mean ± SD of the mean value.

CONFLICT OF INTEREST

The authors state no conflict of interest.

SUPPLEMENTARY MATERIAL

Figure S1. Purification of DCs.

REFERENCES

Akbari O, DeKruyff RH, Umetsu DT (2001) Pulmonary dendritic cells producing IL-10 mediate tolerance induced by respiratory exposure to antigen. *Nat Immunol* 2:725–31

Annacker O, Pimenta-Araujo R, Burlen-Defranoux O, Barbosa TC, Cumano A, Bandeira A (2001) CD25+ CD4+ T cells regulate the expansion of peripheral CD4 T cells through the production of IL-10. *J Immunol* 166:3008–18

Atarashi K, Kabashima K, Akiyama K, Tokura Y (2007) Stimulation of Langerhans cells with ketoprofen plus UVA in murine photocontact dermatitis to ketoprofen. *J Dermatol Sci* 47:151–9

Denys A, Udalova IA, Smith C, Williams LM, Ciesielski CJ, Campbell J *et al.* (2002) Evidence for a dual mechanism for IL-10 suppression of TNF-alpha production that does not involve inhibition of p38 mitogen-activated protein kinase or NF-kappa B in primary human macrophages. *J Immunol* 168:4837–45

Dournon C, Membre H, Bautz A (2001) Sex reversal of germ cell gametogenesis in chimeras of *Pleurodeles waltl* (urodele amphibian): genetic and immunogenetic demonstration using tolerance or rejection of skin grafts. *Dev Growth Differ* 43:97–106

Elmets CA, Bergstresser PR, Tigelaar RE, Wood PJ, Streilein JW (1983) Analysis of the mechanism of unresponsiveness produced by haptens painted on skin exposed to low dose ultraviolet radiation. *J Exp Med* 158:781–94

Flacher V, Bouschbacher M, Verronese E, Massacrier C, Sisirak V, Berthier-Vergnes O *et al.* (2006) Human Langerhans cells express a specific TLR profile and differentially respond to viruses and Gram-positive bacteria. *J Immunol* 177:7959–67

Ghoreishi M, Dutz JP (2006) Tolerance induction by transcutaneous immunization through ultraviolet-irradiated skin is transferable through CD4+CD25+ T regulatory cells and is dependent on host-derived IL-10. *J Immunol* 176:2635–44

Girolomoni G, Gisondi P, Ottaviani C, Cavani A (2004) Immunoregulation of allergic contact dermatitis. *J Dermatol* 31:264–70

Goldszmid RS, Idoyaga J, Bravo AI, Steinman R, Mordoh J, Wainstok R (2003) Dendritic cells charged with apoptotic tumor cells induce long-lived protective CD4+ and CD8+ T cell immunity against B16 melanoma. *J Immunol* 171:5940–7

Groux H (2003) Type 1 T-regulatory cells: their role in the control of immune responses. *Transplantation* 75:8S–12S

Henri S, Vremec D, Kamath A, Waithman J, Williams S, Benoist C *et al.* (2001) The dendritic cell populations of mouse lymph nodes. *J Immunol* 167:741–8

Huang FP, Platt N, Wykes M, Major JR, Powell TJ, Jenkins CD *et al.* (2000) A discrete subpopulation of dendritic cells transports apoptotic intestinal epithelial cells to T cell areas of mesenteric lymph nodes. *J Exp Med* 191:435–44

Inaba K, Pack M, Inaba M, Sakuta H, Isdell F, Steinman RM (1997) High levels of a major histocompatibility complex II-self peptide complex on dendritic cells from the T cell areas of lymph nodes. *J Exp Med* 186:665–72

Kabashima K, Murata T, Tanaka H, Matsuoka T, Sakata D, Yoshida N *et al.* (2003) Thromboxane A2 modulates interaction of dendritic cells and T cells and regulates acquired immunity. *Nat Immunol* 4:694–701

Kang K, Gilliam AC, Chen G, Tootell E, Cooper KD (1998) In human skin, UVB initiates early induction of IL-10 over IL-12 preferentially in the expanding dermal monocytic/macrophagic population. *J Invest Dermatol* 111:31–8

Kaplan DH, Jenison MC, Saeland S, Shlomchik WD, Shlomchik MJ (2005) Epidermal Langerhans cell-deficient mice develop enhanced contact hypersensitivity. *Immunity* 23:611–20

Katz SI, Tamaki K, Sachs DH (1979) Epidermal Langerhans cells are derived from cells originating in bone marrow. *Nature* 282:324–6

Kissenpfennig A, Henri S, Dubois B, Laplace-Builhe C, Perrin P, Romani N *et al.* (2005) Dynamics and function of Langerhans cells *in vivo*: dermal dendritic cells colonize lymph node areas distinct from slower migrating Langerhans cells. *Immunity* 22:643–54

Lin ZQ, Kondo T, Ishida Y, Takayasu T, Mukaida N (2003) Essential involvement of IL-6 in the skin wound-healing process as evidenced by delayed wound healing in IL-6-deficient mice. *J Leukoc Biol* 73:713–21

Loser K, Mehling A, Loeser S, Apelt J, Kuhn A, Grabbe S *et al.* (2006) Epidermal RANKL controls regulatory T-cell numbers *via* activation of dendritic cells. *Nat Med* 12:1372–9

Loser K, Mehling A, Loeser S, Apelt J, Kuhn A, Grabbe S *et al.* (2007) Epidermal RANKL controls regulatory T-cell numbers *via* activation of dendritic cells. *Nat Med* 12:1372–9

Lutz MB, Schuler G (2002) Immature, semi-mature and fully mature dendritic cells: which signals induce tolerance or immunity? *Trends Immunol* 23:445–9

Menger MD, Vollmar B (2004) Surgical trauma: hyperinflammation versus immunosuppression? *Langenbecks Arch Surg* 389:475–84

Min WP, Zhou D, Ichim TE, Strejan GH, Xia X, Yang J *et al.* (2003) Inhibitory feedback loop between tolerogenic dendritic cells and regulatory T cells in transplant tolerance. *J Immunol* 170:1304–12

Rivas JM, Ullrich SE (1992) Systemic suppression of delayed-type hypersensitivity by supernatants from UV-irradiated keratinocytes. An essential role for keratinocyte-derived IL-10. *J Immunol* 149:3865–71

Roelofs-Haarhuis K, Wu X, Nowak M, Fang M, Artik S, Gleichmann E (2003) Infectious nickel tolerance: a reciprocal interplay of tolerogenic APCs and T suppressor cells that is driven by immunization. *J Immunol* 171:2863–72

Romani N, Holzmann S, Tripp CH, Koch F, Stoitzner P (2003) Langerhans cells—dendritic cells of the epidermis. *APMIS* 111:725–40

Schwarz A, Maeda A, Wild MK, Kernebeck K, Gross N, Aragane Y *et al.* (2004) Ultraviolet radiation-induced regulatory T cells not only inhibit the induction but can suppress the effector phase of contact hypersensitivity. *J Immunol* 172:1036–43

Shevach EM (2001) Certified professionals: CD4(+)CD25(+) suppressor T cells. *J Exp Med* 193:F41–6

Shreedhar V, Giese T, Sung VW, Ullrich SE (1998) A cytokine cascade including prostaglandin E2, IL-4, and IL-10 is responsible for UV-induced systemic immune suppression. *J Immunol* 160:3783–9

Silberberg-Sinakin I, Thorbecke GJ (1980) Contact hypersensitivity and Langerhans cells. *J Invest Dermatol* 75:61–7

Simkin GO, Tao JS, Levy JG, Hunt DW (2000) IL-10 contributes to the inhibition of contact hypersensitivity in mice treated with photodynamic therapy. *J Immunol* 164:2457–62

Steinman RM, Turley S, Mellman I, Inaba K (2000) The induction of tolerance by dendritic cells that have captured apoptotic cells. *J Exp Med* 191:411–6

Stingl G, Tamaki K, Katz SI (1980) Origin and function of epidermal Langerhans cells. *Immunol Rev* 53:149–74

Takahashi T, Kuniyasu Y, Toda M, Sakaguchi N, Itoh M, Iwata M *et al.* (1998) Immunologic self-tolerance maintained by CD25+CD4+ naturally anergic and suppressive T cells: induction of autoimmune disease by breaking their anergic/suppressive state. *Int Immunol* 10:1969–80

Takashima A (1995) UVB-dependent modulation of epidermal cytokine network: roles in UVB-induced depletion of Langerhans cells and dendritic epidermal T cells. *J Dermatol* 22:876–87

Taylor PA, Noelle RJ, Blazar BR (2001) CD4(+)CD25(+) immune regulatory cells are required for induction of tolerance to alloantigen *via* costimulatory blockade. *J Exp Med* 193:1311–8

Thorstenson KM, Khoruts A (2001) Generation of anergic and potentially immunoregulatory CD25+CD4 T cells *in vivo* after induction of peripheral tolerance with intravenous or oral antigen. *J Immunol* 167:188–95

Tokura Y, Yagi J, O'Malley M, Lewis JM, Takigawa M, Edelson RL *et al.* (1994) Superantigenic staphylococcal exotoxins induce T-cell proliferation in the presence of Langerhans cells or class II-bearing keratinocytes and stimulate keratinocytes to produce T-cell-activating cytokines. *J Invest Dermatol* 102:31–8

Yagi H, Tokura Y, Wakita H, Furukawa F, Takigawa M (1996) TCRV beta 7+ Th2 cells mediate UVB-induced suppression of murine contact photosensitivity by releasing IL-10. *J Immunol* 156:1824–31

Yasuda H, Murayama M, Yamamoto O, Asahi M (1996) Contact hypersensitivity is suppressed after sensitisation by dinitrofluorobenzene of early stage iso-skin grafts. *Scand J Plast Reconstr Surg Hand Surg* 30:169–75

Zhang X, Izikson L, Liu L, Weiner HL (2001) Activation of CD25(+)CD4(+) regulatory T cells by oral antigen administration. *J Immunol* 167: 4245–53

In the light of our patient's history, symptoms and clinical presentation we diagnosed AGEP following the intake of moxifloxacine. After discontinuation of the antibiotic and intravenous administration of corticosteroids (100 mg prednisolone daily) and antihistaminics (30 mg diphenhydramine hydrochloride twice a day), the rash cleared with typical generalized desquamation within one week. A consecutive patch test with moxifloxacine remained negative. A provocation test with the drug was not performed.
Recent reports suggest an association between the administration of moxifloxacine and elevated liver enzymes, potentially ending in hepatitis fulminans and Stevens-Johnson-Syndrome or TEN (toxic epidermal necrolysis). In this regard our patient remained without relevant pathological findings. AGEP is usually caused by a large variety of drugs, including antibiotics (ß-lactams, pristinamycine, co-trimoxazole, metronidazole), antifungal agents (nystatin, terbinafine, fluconazole, amphotericin B), carbamazepine, hydroxy-chloroquine, azathioprine, diltiazem, nimesulide, non-ionic contrast media and others [1, 3]. Occasional cases of acute pustular drug reactions after the intake of other quinolone antibacterial agents have already been reported [4-6]. Our case is the first description in the literature of AGEP after treatment with moxifloxacine. ■

Acknowledgments. *Conflict of interest: none. Financial support: none.*

Department of Dermatology and Venerology, Hospital Hietzing, Wolkersbergenstr.1, 1130 Vienna, Austria
<michael.schierl@wienkav.at>

Robert FELDMANN
Michael SCHIERL
Paul G. SATOR
Friedrich BREIER
Andreas STEINER

1. Sidoroff A, Dunant A, Viboud C, *et al.* Risk factors for acute exanthematous pustulosis (AGEP) - results of a multi-national case-control study (EuroSCAR). *Br J Dermatol* 2007; 157: 989-96.
2. Ofuji S, Yamamoto O. Acute generalized exanthematous pustulosis associated with a parvovirus B19 infection. *J Dermatol* 2007; 34: 121-3.
3. Roujeau JC, Bioulac-Sage P, Bourseau C, *et al.* Acute generalized exanthematous pustulosis. Analysis of 63 cases. *Arch Dermatol* 1991; 127: 1333-8.
4. Hausermann P, Scherer K, Weber M, Bircher AJ. Ciprofloxacin-induced acute generalized exanthematous pustulosis mimicking bullous drug eruption confirmed by a positive patch test. *Dermatology* 2005; 211: 277-80.
5. Allegue F, Rodríguez Pascual C, Cameselle Teijeiro J, Olcoz MT. Pustular eruption induced by norfloxacin. *Med Clin (Barc)* 1992; 99: 274-5.
6. Tsuda S, Kato K, Karashima T, Inou Y, Sasai Y. Toxic pustuloderma induced by ofloxacin. *Acta Derm Venereol* 1993; 73: 382-4.

doi:10.1684/ejd.2008.0585

Cisplatin-induced acral erythema

Chemotherapy-induced acral erythema (CAE) is a cutaneous reaction associated with the use of various systemic chemotherapeutic agents, usually administered at high doses. Since 1982, when CAE was first described, it has been reported under a variety of names, such as palmoplantar erythema, palmoplantar erythrodysaesthesia syndrome and hand-foot syndrome. CAE tends to occur in patients with malignancies, especially those receiving cumulative high-dose chemotherapy with concomitant irradiation and bone-marrow transplantation. The incidence of acral erythema during chemotherapy is about 2% [1] and the main agents responsible are fluorouracil and doxorubicine, followed by docetaxel, pacritaxel, methotrexate, vinorelvine, gemcitabine, cytarabine and cyclophosphamide [1, 2]. We report a patient who developed an erythematous eruption on the palms after systemic administrations of cisplatin, and review the literature of cisplatin as the causative agent of CAE.
A 35-year-old woman was diagnosed as having cervical cancer. After hysterectomy, a combination therapy with irradiation (30 Gy/total) and cisplatin (30 mg/m^2) was started. Cisplatin was administered intravenously through her left cephalic vein. At night on the initial day of the treatment, she felt a burning pain in her reddish swollen forearm. The swelling subsided within a day by topical application of betamethasone 1 g per day. However, on the 6th day of chemotherapy, she again developed swelling on her left upper limb and was referred to us.
On physical examination, her left forearm was swollen and slightly reddish. There was symmetrical erythema on the bilateral palms extending to the palmar surface of the fingers *(figures 1A, B)*. The eruption consisted of multiple, salmon-pink, faintly demarcated, non-tender lesions. No eruption was noted on the dorsum of hands and fingers. Laboratory data revealed no leucocytosis or peripheral eosinophilia. We did not perform any skin tests for ethical reasons, because of the cytotoxic properties. Drug-

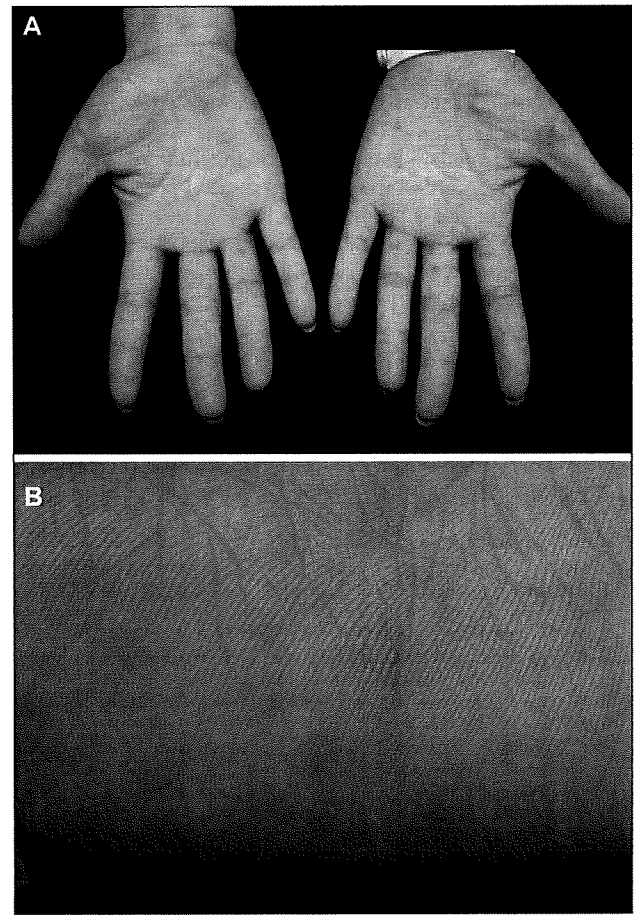

Figure 1. Acral erythematous eruption on both palms **(A)**, showing multiple, demarcated, salmon-pink lesions **(B)**.

induced lymphocyte stimulation testing was tried, but it was difficult to evaluate its antigenicity, since lymphocytes were incapable of surviving during culture with cisplatin. A tentative diagnosis of drug eruption was made; she stopped taking cisplatin and her eruption was completely resolved in a week without any treatment.

A biopsy specimen from a palmar lesion revealed a perivascular mild infiltrate of lymphocytes and a few eosinophils in the dermis with mildly acanthotic epidermis. There were no epidermal necrotic cells or dermal inflammatory cells invading into the eccrine glands.

Although cisplatin is widely used for the treatment of various tumors, cisplatin-induced acral erythema has been reported in only four cases [2-4]. All patients developed symmetrical erythema of the palms and fingers and/or soles, and the eruptions were resolved by discontinuing cisplatin. However, there are clinical and histological differences among these cases. First, acral erythema occurred only one day after the initiation of chemotherapy in our case, while it appeared 3 months after the initiation in another patient [2]. Second, the lesional sites were slightly different between the cases. Third, the infiltrates consisted of lymphocytes [2], or neutrophils [4]. Finally, lichenoid or vesicular changes in the epidermis were present in two cases [2, 4] but not in our case.

The occurrence of CAE depends on various factors, which may contribute the typical localization to the palms and soles, including elevated drug concentration in eccrine glands, rapid cell proliferation, regional temperature gradient, gravitational forces, and vasculature anatomy [5]. Thus, it is likely that CAE is a toxic but not allergic reaction. Because the onset of CAE was soon after administration, our case also supports some toxic mechanism underlying CAE.

It may be noted that three out of the four reported cases are Japanese, and some ethnic genetic background might influence on the susceptibility of CAE to cisplatin. The polymorphisms for certain drug transporter genes, such as Multi drug resistance 1, might underlie the ethnic variation [6]. ■

Acknowledgements. Financial support: none. Conflict of interest: none.

Department of Dermatology, University of Occupational and Environmental Health, Japan, 1-1 Iseigaoka Yahatanishi-ku, Kitakyushu 807-8555, Japan
<fkmc-shk@med.uoeh-u.ac.jp>

Shoko FUKAMACHI
Motonobu NAKAMURA
Yoshiki TOKURA

1. Hueso L, Sanmartin O, Nagore E, *et al.* Chemotherapy-induced acral erythema: a clinical and histopathologic study of 44 cases. *Actas Dermosifiliogr* 2008; 99: 281-90.
2. Vakalis D, Ioannides D, Lazaridou E, *et al.* Acral erythema induced by chemotherapy with cisplatin. *Br J Dermatol* 1998; 139: 750-1.
3. Kimura K. Cisplatin-induced acral erythema. *Rinsho Derma (Tokyo)* 1988; 30: 1379-83.
4. Yamada T, Tanaka R, Kusuda Y, Fujisawa M. Chemotherapy-induced acral erythema with vesicles on soles. *Jpn J Dermatol* 2005; 115: 1643.
5. Lorusso D, Di Stefano A, Carone V, *et al.* Pegylated liposomal doxorubicin-related palmar-plantar erythrodysesthesia ('hand-foot' syndrome). *Ann Oncol* 2007; 18: 1159-64.
6. Sohn JW, Lee SY, Lee SJ, *et al.* MDR1 polymorphisms predict the response to etoposide-cisplatin combination chemotherapy in small cell lung cancer. *Jpn J Clin Oncol* 2006; 36: 137-41.

doi:10.1684/ejd.2008.0586

Successful treatment of cutaneous leishmaniasis by photodynamic therapy and cryotherapy

Cutaneous leishmaniasis (CL) sometimes brings a therapeutic problem. The treatments of Old World cutaneous leishmaniasis include cryotherapy [1], heat therapy, itraconazole [2], pentavalent antimony compounds, amphotericin B and other antimycotic drugs, topical and intralesional application of paramomycin, and in recent years also photodynamic therapy (PDT) [3-5]. Lesions of CL heal spontaneously over several months to 2-3 years, and therapy is not always essential. Nevertheless, treatment is indicated in spreading multiple lesions and when the lesion is located on the face and exposed areas of the extremities.

A 39-year-old man was referred to us with multiple lesions similar to furunculosis, which had occured 3 months previous without healing after topical steroid therapy. He was a keen diver and the lesions developed 4 weeks after his last return from vacation in Croatia. The examination revealed a healthy man with 9 slightly tender nodules and plaques of bright pink-reddish colour, sized 1 to 4 cm on the forearms, neck, and thigh. They periodically developed some blistering on the surface *(figure 1A)*. The diagnosis of cutaneous leishmaniasis was confirmed by a biopsy specimen. *Leishmania* bodies were present in the macrophages as well as extracellularily. No microorganisms were seen in PAS staining and in sections stained to show acid-fast organisms. A culture was not performed.

The following treatment was introduced: Five lesions were treated with PDT whereas the other 4 lesions were treated with cryotherapy. Before initiation of PDT, the crusts and scales were mechanically removed. Then, 20% ALA in gel (hydrochloride form) was applied on the lesions in a 1 mm thick layer. The areas were covered with an occlusive dressing for 3 hours after which the gel was washed off using 0.9 saline solution. Each lesion was illuminated with non-coherent red light with an emission spectrum of 580 to 680 nm (Medeikonos, Sweden), with a total light dose of 75 J/cm^2 and a light intensity of 88-123 mW/cm^2. The PDT procedure was repeated once a week for six-weeks.

The remaining 4 lesions were treated simultaneously with a hand-held liquid nitrogen spray unit. The liquid nitrogen was applied directly on the lesion from a distance of 2-3 cm for a freezing time of 30 seconds and a thaw of 60 seconds. Double freeze-thaw cycle treatment per session was used. The procedure was performed once a week for five weeks in total.

The lesions treated with the PDT method improved after 4 sessions and after 6 sessions they were healed with only minimal pigmentation and minor central scarring *(figure 1B)*. The lesions treated with cryotherapy healed after 5 applications with slight pigmentation and minor scar formation in the centre of the lesions, too *(figure 1C)*. No biopsies from clinically healed skin were performed after completion of the treatment. In a 12 month follow-up period no signs of reccurence occured.

DOI:10.1111/j.1600-0625.2009.00899.x
www.blackwellpublishing.com/EXD

Original Article

Induction of eosinophil- and Th2-attracting epidermal chemokines and cutaneous late-phase reaction in tape-stripped skin

Ayako Onoue, Kenji Kabashima, Miwa Kobayashi, Tomoko Mori and Yoshiki Tokura

Department of Dermatology, University of Occupational and Environmental Health, Yahatanishi-ku, Kitakyushu, Japan
Correspondence: Yoshiki Tokura, MD, PhD, Department of Dermatology, University of Occupational and Environmental Health, 1-1 Iseigaoka, Yahatanishi-ku, Kitakyushu 807-8555, Japan, Tel.: +81 93 691 7445, Fax: +81 93 691 0907, e-mail: tokura@med.uoeh-u.ac.jp

Accepted for publication 27 March 2009

Abstract: Skin barrier damage induces various harmful or even protective reactions in the skin, as represented by enhancement of keratinocyte cytokine production. To investigate whether acute removal of stratum corneum modulates the production of chemokines by epidermal cells, we treated ears of BALB/c and C57BL/6 mice by tape-stripping, or acetone-rubbing as a control of acute barrier disruption procedure. There was no difference between the tape-stripped and acetone-rubbed skin sites in the increased and recovered levels of transepidermal water loss. The mRNA expression levels of all the chemokines tested, including Th1 chemokines (CXCL10, CXCL9 and CXCL11), Th2 chemokines (CCL17 and CCL22) and eosinophil chemoattractant (CCL5), were higher in the epidermal cells from BALB/c than in those of C57BL/6 mice. In particular, CCL17, CCL22 and CCL5 were remarkably elevated in BALB/c mice and augmented by tape-stripping more markedly than acetone-rubbing, whereas Th1 chemokines were enhanced by acetone-rubbing more remarkably. Tape-stripping induced dermal infiltration of eosinophils in BALB/c but not C57BL/6 mice. In a contact hypersensitivity model, where BALB/c mice were sensitized on the abdomen and challenged on the ears with fluorescein isothiocyanate, mice exhibited higher ear swelling responses at the late-phase as well as delayed-type reactions, when challenged *via* the tape-stripped skin. The challenge *via* tape-stripped skin augmented the expression of IL-4 and CCR4 in the skin homogenated samples, indicating infiltration of Th2 cells. These findings suggest that acute barrier removal induces the expression of Th2 and eosinophil chemokines by epidermal cells and easily evokes the late phase reaction upon challenge with antigen.

Key words: barrier disruption – chemokines – eosinophil – late-phase reaction – tape stripping

Please cite this paper as: Induction of eosinophil- and Th2-attracting epidermal chemokines and cutaneous late-phase reaction in tape-stripped skin. Experimental Dermatology 2009.

Introduction

Stratum corneum, which is the outermost, cornified layer of the epidermis, serves as skin barrier and protects from external micro-organisms and chemicals and even sunlight radiation (1). When this barrier is destroyed or removed, these hazardous invaders penetrate through the skin. Upon exposure to the agents, however, the epidermis produces or expresses various protective molecules such as cytokines (2), anti-bacterial peptides (3) and cornification-promoting molecules (4).

There are both the acute and chronic disruption procedures for experimental impairment of the skin barrier in rodents (5,6). Furthermore, the acute barrier disruption has been performed by two different procedures in mice, stripping with scotch tape and rubbing with acetone cotton (2). These two treatment modalities stimulate keratinocytes to produce cytokines, such as interleukin-1α, tumor necrosis factor-α and granulocyte/macrophage colony stimulating factor and enhance contact hypersensitivity when a hapten is applied on the barrier-disrupted skin at either of the sensitization or challenge phase (2). However, the pathophysiological significance of barrier disruption in skin infiltration of inflammatory cells remains to be clarified. Given that barrier damage induces the release of chemokines from the epidermis, it is possible that certain inflammatory cells are present or prone to infiltrate in the barrier-disrupted skin.

Although both tape-stripping and acetone-rubbing have been categorized as the procedure of acute barrier disruption, it remains unknown whether these two treatments exert the same effect on the production of chemokines by epidermal cells and the resultant infiltration of leucocytes in the skin. While tape-stripping mechanically removes the cornified layer of the epidermis, acetone-rubbing chemically deletes sphingolipids, such as ceramide, existing

between the layers of corneocytes (2). Therefore, it seems that tape-stripping resembles scratching and more likely reflects clinical conditions. For example, the tape-stripped skin may share the chemokine production status with the skin of pruritic disorders such as atopic dermatitis.

This study was aimed to investigate whether tape-stripping modulates the production of chemokines by epidermal cells in a comparison with acetone-rubbing. We treated the ears of mice by tape-stripping or acetone-rubbing and examined the expression/production of chemokines by epidermal cells (ECs), the infiltration of inflammatory cells and the late-phase and delayed-type hypersensitivities. In addition, it was necessary that Th2- and Th1-preponderant mouse strains, BALB/c and C57BL/6 (B6) mice respectively, were compared in the effects of tape-stripping. Results suggest that tape-stripping induces the production of Th2 cell- and eosinophil-associated chemokines more markedly than acetone-rubbing in BALB/c mice and this skewed elaboration of chemokines determines the infiltration of Th2 cells and eosinophils and the cutaneous hypersensitivity responses.

Materials and methods

Animals and chemicals

Seven to 10 week-old female BALB/c and B6 mice were purchased from Japan SLC (Hamamatsu, Japan). These mice were maintained in the Laboratory Animal Research Center in University of Occupational and Environmental Health under specific pathogen-free conditions. All animal experiments were performed according to the guidelines for the care and use of animals approved by our university. Fluorescein isothiocyanate (FITC) was obtained from Sigma Chemical Co. (St Louis, MO).

Acute barrier disruption procedures

The procedures were reported previously (2). Mechanical barrier disruption was achieved by stripping both sides of the earlobe with cellophane tape (Nichiban, Tokyo, Japan) seven times. This manipulation effectively removed stratum corneum without hazardous haemorrhagic change. For chemical disruption, both sides of the earlobe were gently rubbed for 30 s with cotton ball dipped in absolute acetone. These two disruption procedures were performed in different mice.

Transepidermal water loss (TEWL)

Immediately (time 0) and at various times after barrier disruption with tape-stripping and acetone-rubbing, TEWL was measured in the treated and untreated earlobes with Vapa Scan AS-VT100RS (Asahi Biomed, Yokohama, Japan) in the measurement room which had a temperature of 23–25°C and a relative humidity of 49–54%.

Preparation of epidermal cells (ECs)

Skin sheets from earlobes untreated or treated with tape or acetone 6, 12 and 24 h before were floated in 0.2% trypsin (Difico Laboratories, Detroit, MI, USA), dissolved in phosphate-buffered saline (PBS; pH 7.4) for 1 h at 37°C (7). Epidermis was then separated from dermis with forceps in PBS supplemented with 10% of fetal calf serum (Gibco, Carlsbad, CA, USA). EC suspensions were prepared by pipetting and filtration through nylon mesh (pore size, 77 mm) and included 97% keratinocytes and 2% Langerhans cells as assessed using flow cytometric analysis with anti-I-A antibody (8).

Real-time quantitative PCR analysis of ECs

For detection of epidermal chemokines, EC suspensions were used as samples. Total cellular RNA of ECs was extracted with the RNA extraction kit (Promega, Madison, WI, USA) from freshly prepared skin samples. There was no remarkable difference between the acetone-rubbed and tape-stripped samples in the amounts of extracted RNA. RNA was then reverse transcribed and amplified by random hexamer in single tube assay using the TaqMan Reverse Transcription Reagents (Applied Biosystems, Foster City, CA, USA) with gene-specific sense and antisense primers and a detection probe labelled on the 5′ end with the reporter dye 6-FAM. Primers and probes were obtained from TaqMan Gene Expression Assays Inventories (Applied Biosystems) for CXCL10/IP-10, CXCL9/Mig, CXCL11/I-TAC, CCL17/TARC, CCL22/MDC and CCL5/RANTES. Using the ABI Prism 7000 sequence detection systems (Applied Biosystems), duplicate samples were reverse transcribed and amplified under the following consecutive steps: 2 min at 50°C, 10 min at 95°C, followed by 50 amplification cycles of 15 s at 95°C and 1 min at 60°C. Sequence-specific amplification was detected as an increased fluorescent signal of 6-FAM exceeding the threshold limit during the amplification cycle. Quantification of gene-specific message levels was determined by comparing fluorescence intensity from unknown RNA samples to the fluorescence intensity of standard curve generated from control mRNA levels. Amplification of the gene for mouse β-actin was performed on all samples to control interspecimen variations in RNA amounts. The result for each gene was normalized to the quantity of mouse β-actin detected in the sample. Levels of gene-specific message were graphed as normalized message units as determined from standard curve.

Enzyme-linked immunosorbent assay (ELISA)

Chemokine levels were studied using ELISA method. Dispersed ECs from barrier-disrupted or untreated earlobes were cultured at 1×10^6 per ml in Eagle's minimal essential medium containing 10% fetal calf serum, 1% streptomycin